AD-A166 274 EXPERIMENTAL STUDY OF ELECTRONIC STATES AT METAL-DIELECTRIC INTERFACES..(U) CORNELL UNIV ITHACA NY LAB OF ATOMIC AND SOLID STATE PHYSICS.. A J SIEVERS

1/1

UNCLASSIFIED 23 DEC 85 AFOSR-TR-86-0080 AFOSR-81-0121 F/G 7/4 NL

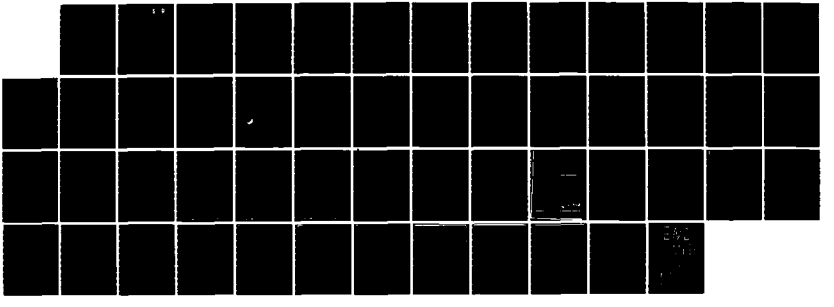

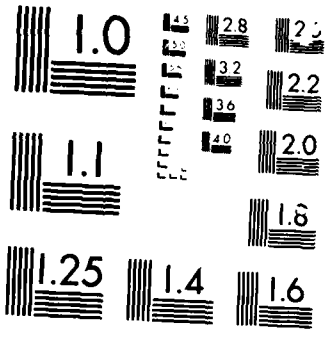

MICROCOPY RESOLUTION TEST CHART

(2)

(UNCLASSIFIED)
SECURITY CLASSIFICATION OF THIS PAGE

REPORT DOCUMENTATION PAGE

REPORT SECURITY CLASSIFICATION: (UNCLASSIFIED)	1b. RESTRICTIVE MARKINGS: D
SECURITY CLASSIFICATION AUTHORITY: open	3. DISTRIBUTION/AVAILABILITY OF REPORT: Approved for public release; distribution unlimited.
DECLASSIFICATION/DOWNGRADING SCHEDULE:	
PERFORMING ORGANIZATION REPORT NUMBER(S):	5. MONITORING ORGANIZATION REPORT NUMBER(S): AFOSR-TR- 86-0080
NAME OF PERFORMING ORGANIZATION: Cornell University	6b. OFFICE SYMBOL (If applicable):
	7a. NAME OF MONITORING ORGANIZATION: AFOSR
ADDRESS (City, State and ZIP Code): Clark Hall, Cornell University, Ithaca, NY 14850-2501	7b. ADDRESS (City, State and ZIP Code): Bolling AFB, Bldg. 410, Washington, D.C. 20332
8a. NAME OF FUNDING/SPONSORING ORGANIZATION: AFOSR	8b. OFFICE SYMBOL (If applicable): NE
	9. PROCUREMENT INSTRUMENT IDENTIFICATION NUMBER: AFOSR 81-0121
8c. ADDRESS (City, State and ZIP Code): Bolling AFB, Bldg. 410, Washington, D.C. 20332	10. SOURCE OF FUNDING NOS.

PROGRAM ELEMENT NO.	PROJECT NO.	TASK NO.	WORK UNIT NO.
(61102) F	2306	B2	

11. TITLE (Include Security Classification): Experimental Study of Electronic States at Metal Dielectric Interfaces

12. PERSONAL AUTHOR(S): A. J. Sievers

13a. TYPE OF REPORT	13b. TIME COVERED	14. DATE OF REPORT (Yr., Mo., Day)	15. PAGE COUNT
Final Technical	FROM 2/2/81 TO 5/31/85	12/23/85	48

16. SUPPLEMENTARY NOTATION

17. COSATI CODES			18. SUBJECT TERMS (Continue on reverse if necessary and identify by block number)
FIELD	GROUP	SUB. GR.	Electromagnetic; Electronic; Broadband

19. ABSTRACT (Continue on reverse if necessary and identify by block number)

Novel high resolutions electromagnetic wave techniques have been used in the optical, infrared and far infrared spectral regions to explore the electronic states at metaldielectric interfaces. Because infrared surface plasmons on metal surfaces propagate for many wavelengths, a measurement of the transmission of these surface excitations has proven to be a sensitive probe of the surface itself. Both broadband and single frequency generation techniques have been developed. Reconstructed surfaces as well as surfaces covered with a chemisorbed atomic monolayer or a thin dielectric or molecular film have been investigated with these new methods.

20. DISTRIBUTION/AVAILABILITY OF ABSTRACT	21. ABSTRACT SECURITY CLASSIFICATION
UNCLASSIFIED/UNLIMITED ☒ SAME AS RPT ☒ DTIC USERS ☐	(UNCLASSIFIED)

22a. NAME OF RESPONSIBLE INDIVIDUAL	22b. TELEPHONE NUMBER (Include Area Code)	22c. OFFICE SYMBOL
A. J. Sievers (Prof. Kenneth Mobley) A. J. Sievers	(607) 256-6422	NE

DD FORM 1473, 83 APR — EDITION OF 1 JAN 73 IS OBSOLETE.

(UNCLASSIFIED)

AFOSR-TR- 86-0080

FINAL TECHNICAL REPORT

February 2, 1981 - May 31, 1985

Experimental Study of Electronic States at Metal-Dielectric Interfaces

Submitted to: AFOSR/NE
Att: Capt. G. T. Rosalia

Submitted by: Cornell University
Ithaca, NY 14853

Principal Investigator: A. J. Sievers
Prof. of Physics
Lab. of Atomic and
Solid State Physics

Table of Contents

I. ABSTRACT

Novel high resolutions electromagnetic wave techniques have been used in the optical, infrared and far infrared spectral regions to explore the electronic states at metal dielectric interfaces. Because infrared surface plasmons on metal surfaces propagate for many wavelengths, a measurement of the transmission of these surface excitations has proven to be a sensitive probe of the surface itself. Both broadband and single frequency generation techniques have been developed. Reconstructed surfaces as well as surfaces covered with a chemisorbed atomic monolayer or a thin dielectric or molecular film have been investigated with these new methods.

II. OBJECTIVES

A variety of different kinds of electromagnetic experiments have been developed to provide new information about the excitation properties of electronic states at interfaces. Infrared surface electromagnetic wave measurements on a variety of metals using the edge coupling technique enabled us to develope the first quantitative IR surface probe. The method was first used to measure Ge coated Ag and Au metals and then later a single crystal tungsten surface in ultrahigh vacuum conditions. The large changes in the surface electromagnetic wave attenuation coefficient upon adsorption of diatomic gases on the tungsten surface have been identified as adsorbate induced changes in conduction electron scattering at the surface. These measurements provide the first infrared signature of adsorbate-induced surface reconstruction. While making these measurements a new interference phenomenon was discovered on clean metal surfaces which involves both plane electromagnetic waves and infrared surface plasmons. The identification of the interference minimum gives the first quantitative measurement of the surface plasmon index of refraction and hence the carrier number density at the metal surface. Optical evanescent wave measurements on silver-dielectric interfaces show that surface electrodynamic processes are more important in this frequency region than previously expected. Far infrared transmission measurements on metal-dielectric composites demonstrate that the anomalously large absorption observed when 100A metal particles are superconducting is due to particle clumping and is not an intrinsic property of the particle surface.

III. ACCOMPLISHMENTS

Our progress during the past three years is highlighted by three novel types of electromagnetic experiments on metals. Optical measurements show that surface electrodynamic processes are more important than previously expected, infrared measurements provide the first direct measurement of both the real and imaginary parts of the surface impedance and far infrared measurements demonstrate that the anomalous far infrared absorptivity of 100A metal particles is due to particle clumping.

A) Optical Properties of Ag Mirrors

The optical data for the noble metals at frequencies below the interband absorption edge are accurately characterized by the free electron Drude model.[1] The real and imaginary parts of the metal dielectric function can be written

$$\varepsilon_1 \simeq \varepsilon_\infty - \frac{\omega_p^2}{\omega^2}, \tag{1}$$

$$\varepsilon_2 = \frac{\varepsilon_\infty - \varepsilon_1}{\omega\tau} \tag{2}$$

in the limit where $\omega\tau \gg 1$. The three parameters of the model are ε_∞, the corepolarizability and interband transition contribution to the dc dielectric constant, $\omega_p^2 = 4\pi Ne^2/m$, the plasma frequency squared and τ^{-1}, the electron scattering rate. Both τ^{-1} and ω_p are found to vary depending on the sample preparation techniques.[2,3]

A consistent explanation of the variations observed for ω_p has not yet been found although the changes are usually assigned to surface morphology. The ω_p's measured for the thin semitransparent Au films investigated by Théye are about 5% larger than the values reported for electropolished bulk samples.[2] Almost the same change in ω_p has been measured by Hodgson for the

internal and external surface of an opaque Au film[4] with the larger ω_p occuring for the film-substrate interface. Since it was known that a thin oxide layer would reduce the apparent value of ε_1 and ε_2 to,[5]

$$\varepsilon_1(\text{app.}) = \left(1 - \frac{2t\omega_p}{c}\,\frac{\varepsilon_{ox}-1}{\varepsilon_{ox}} + O\left(\frac{t\omega_p}{c}\right)^2\right)\varepsilon_1 \tag{3}$$

and

$$\varepsilon_2(\text{app.}) = \left(1 - \frac{3t\omega_p}{c}\,\frac{\varepsilon_{ox}-1}{\varepsilon_{ox}} + O\left(\frac{t\omega_p}{c}\right)^2\right)\varepsilon_2 \tag{4}$$

for $\omega\tau \gg 1$, the discrepancies have usually been blamed on this added ingredient.

More recently, Weber and McCarthy[6,7] confirmed the Au results and showed that a similar effect existed for Ag films. They found that ω_p at the substrate interface was consistently about 5% larger than the ω_p at the air interface. They proposed that this difference could be understood if the metal density near the air interface was several percent below that near the substrate interface. The ubiquitious oxide layer was no longer required to explain the apparent decrease in ε_1 at the air-metal interface. One of the prediction of the variable density model is that if the air is replaced by a dielectric then the apparent decrease in ε_1 should be even larger.

By measuring at eight visible wavelengths ε_1 and ε_2 of an Ag film against air and then against a transparent organic liquid, we find that this idea is not confirmed. Our results for ε_1 are shown in Fig. 1. The measured change has the opposite sign from that given by the variable density model; however, our complete dielectric function still can be described by the Drude model with the well known frequency dependent relaxation time, namely, $\tau^{-1}(\omega) = \tau_0^{-1} + \beta\omega^2$. The interesting results are that $\tau_0^{-1}(\text{liquid}) > \tau_0^{-1}(\text{air})$, $\beta(\text{liquid}) < \beta(\text{air})$ and that the plasma frequency $\omega_p\,(\text{liquid}) > \omega_p(\text{air})$. The

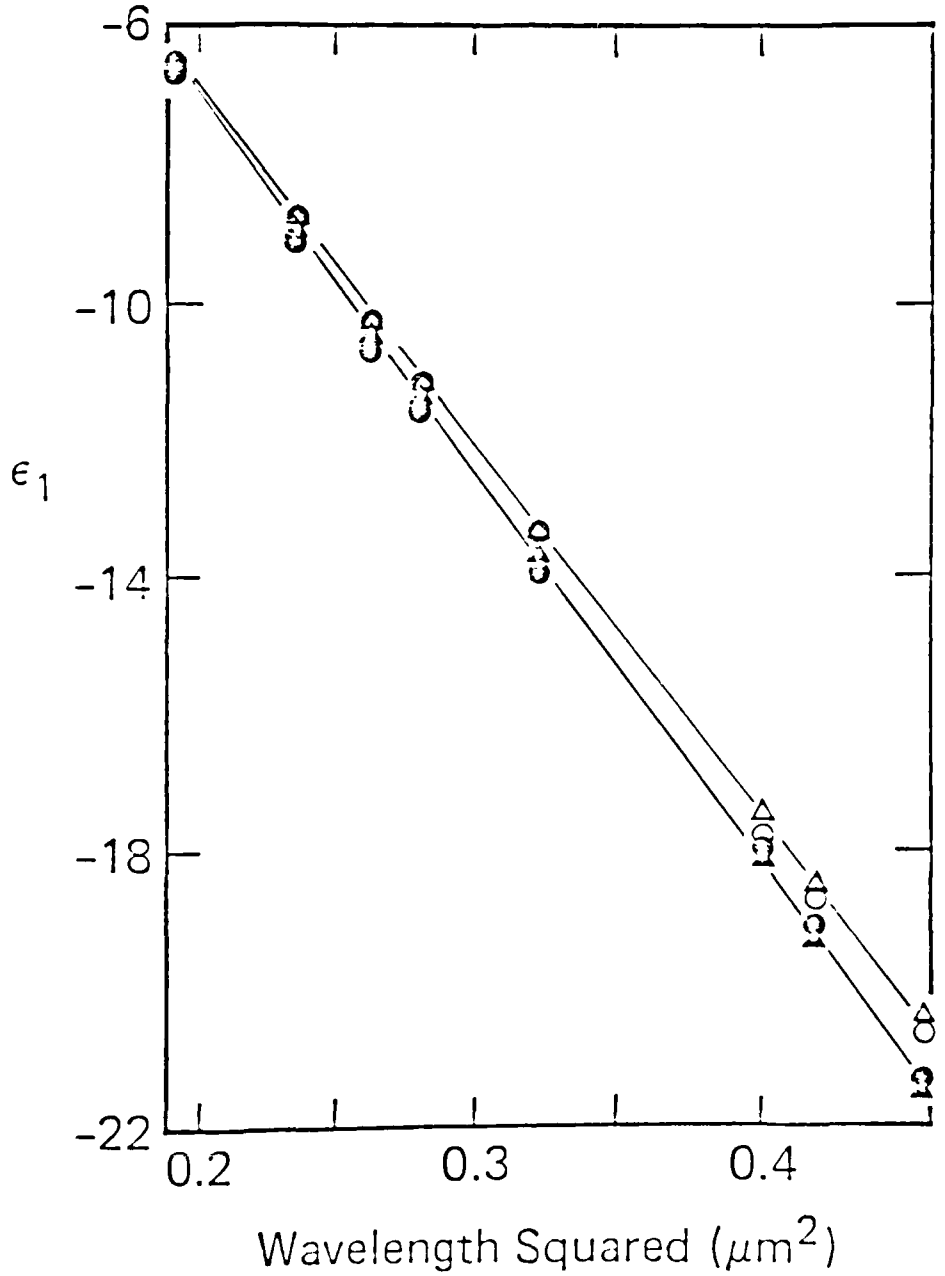

Figure 1. The measured real part of the dielectric function of silver versus wavelength squared for both air Δ and CCl_4 Δ half spaces and air O and hexane O half spaces. The lines are average values and given to clearly show the trends.

fact that β changes, the sign of the change or its magnitude, appear to eliminate all previous models which have been proposed to describe this frequency dependent term. The observed changes in β and ω_p are consistent with the idea of a complex relaxation time whose real and imaginary parts are conneted in a causal way. The index of refraction dependence of the Drude parameters demonstrates that surface electrodynamics must play an important role in determining the optical properties of noble metals.

B. Infrared Surface Electromagnetic Wave Interferometry on Clean W(100).

A few years ago we discovered an interference phenomen on which involved plane electromagnetic waves (PEW's) and infrared surface electromagnetic waves (SEW's) on dielectric coated metal surfaces.[8] We now report the observation of a related interference phenomenon on clean metal surfaces. The interference is demonstrated with a two beam interferometer of fixed optical path and variable frequency. The identification of the interference minimum gives the first direct measurement of the SEW index of refraction and hence the infrared plasma frequency.

SEW's are TM (p-polarized) inhomogeneous surface waves which propagate along a metal/vacuum interface at nearly the velocity of light. For good metallic conductors the infrared surface wave attenuation coefficient is

$$\alpha_s = \omega^2 \rho / 4\pi c \qquad (5)$$

where ω is the frequency, ρ the d.c. resistivity and c the velocity of light. In the same limit the index of refraction of this mode is

$$n_s = 1 + \omega^2 / 2\omega_p{}^2 \qquad (6)$$

where ω_p is the infrared plasma frequency.

Because the SEW wavevector is greater than that of light we use gratings etched into a W(100) surface to couple CO_2 laser radiation to and from SEW's. We find that these grating couplers not only excite the SEW mode but

also excite plane waves at the same frequency. These PEW's are produced in the form of a packet traveling in the forward direction and spreading slowly in width. The SEW travels along the surface with a phase velocity c/n_s while the phase velocity of the PEW's which travel above the surface is c. At the output grating coupler which is a distance ℓ from the input grating the SEW and PEW packet both contribute to the output amplitude; however, these two contributions are no longer in phase. The total intensity of the resultant PEW's launched by the second grating is

$$I = I_s + I_p + 2(I_s I_p)^{1/2} \cos \theta \qquad (7)$$

where $\theta = [(n_s - 1)\ \omega\ell/c + \phi]$ with ϕ a constant. Complete destructive interference occurs when $\theta = (2m + 1)\ \pi$ and $I_s = I_p$. For W(100) and a path lenth of 5 cm the phase is adjusted to destructive interference by varying the CO_2 laser frequency from 900 cm^{-1} to 1070 cm^{-1}. In order to obtain equal intensity in the two arms of the interferometer, the sample temperature is varied. Since $\rho \sim T$ and $I_s \sim \exp(-\alpha_s \ell)$, a modest temperature excursion changes this component by orders of magnitude. The temperature dependences of the intensity for various CO_2 laser frequencies are shown in Fig. 2. For W(100) the interference gives $\hbar\omega_p = 6.9 \pm 0.3$ eV. The Kramers Kronig analysis of reflectivity measurements[9] on W gives $\hbar\omega_p = 6.0$eV. The difference between these two values is much larger than the experimental uncertainties in the SEW measurement.

The infrared SEW interferometer can be realized for poor conductors as well as good ones such as W. If the surface propagation length, ℓ, is made long enough so that a π phase change can occur between the two optical paths, then for any conductor the condition for sufficient SEW intensity at the output is simply $\alpha_s \ell \simeq 3\pi/\omega\tau$ where τ is the electron relaxation time. Thus the interference can be observed as long as the infrared frequency is chosen such that $\omega\tau > 1$.

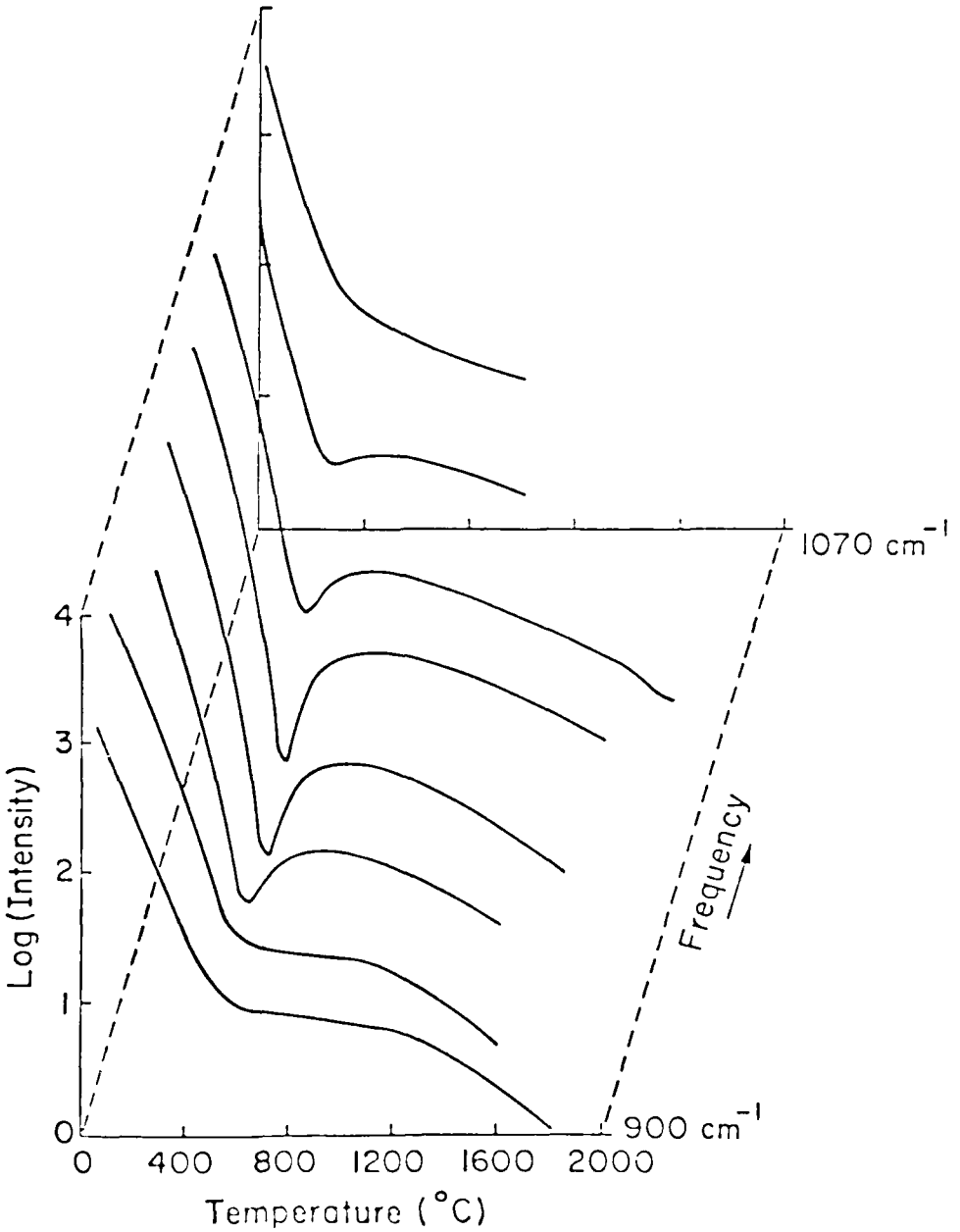

Figure 2. SEW interference signal versus frequency and temperature. The low temperature signal is mainly due to SEW's and the high temperature signal mainly due to PEW's. At temperatures around 400°C the two component intensities are equal in magnitude. The sample is a single crystal of W with <100> faces.

C. Anomalous Far Infrared Absorption by 100A Metal Particle Composites.

The anomalous enhancement by many orders of magnitude of the measured far infrared absorption coefficient of composite materials containing very small metal particles (diameter $\lesssim$ 100Å) with respect to the predictions of simple models is not understood largely due to a lack of well-characterized samples with controllable properties. The configuration of the particles in the samples used in previous investigations, typically a free standing metal smoke[10] or a metal smoke mixed with an alkali halide and pressed into pellets[11,12], was not determined, e.g. with an electron microscope. Thus, the available data do not convincingly support or eliminate either proposed explanations that require clumping[13] or intrinsic mechanisms that can take place in isolated particles.[14]

Recent experiments by Carr, Garland and Tanner[15] on granular superconducting samples consisting of small Sn particles embedded in an alkali halide host have shown additional unusual results. Carr et al. found that not only is the absorption anomalously large in comparison with the predictions of classical theories[16,17] but at frequencies higher than the superconducting gap frequency the composites are more absorbing in the superconducting state than in the normal state. This superconducting behavior is surprising since bulk Sn has smaller electromagnetic absorption in the superconducting state.

Two different kinds of far infrared measurements on composites systsems have now been completed and they demonstrate that particle clumping is the source of both kinds of anomalies.

The first experiment involves measurements on a novel composite material--100Å diameter Ag particles imbedded in a gelatin matrix[18]. For the first time, the particles under study by far infrared spectroscopy can also be examined in situ by transmission electron microscopy. Samples containing

either well-dispersed or agglomerated particles can be prepared. The volume fraction of Ag can be varied over a large range. The experimental far infrared absorption data[10], which are consistent with the Bruggeman model, are shown in Fig. 3. Inspection of this figure demonstrates that the absorption coefficient of materials with well-dispersed particles is not enhanced by several orders of magnitude, if at all. However, we do find that samples containing deliberately agglomerated particles are measured to be stronger absorbers.

The second experiment deals with the study of the far infrared absorption of several types of Sn particle KBr composites which have been subjected to a temperature excursion above the Sn melting point. We find that this simple device drastically decreases the magnitudes of the measured absorption coefficients. The specifics depend on whether or not the particles possess an oxide coating, however, above the gap frequency the superconducting state absorption is no longer larger than the normal state valve. On the grounds that heat treatment should not significantly affect the superconducting properties of isolated particles, we are led also to identify the superconducting anomaly in earlier measurements with particle clustering.

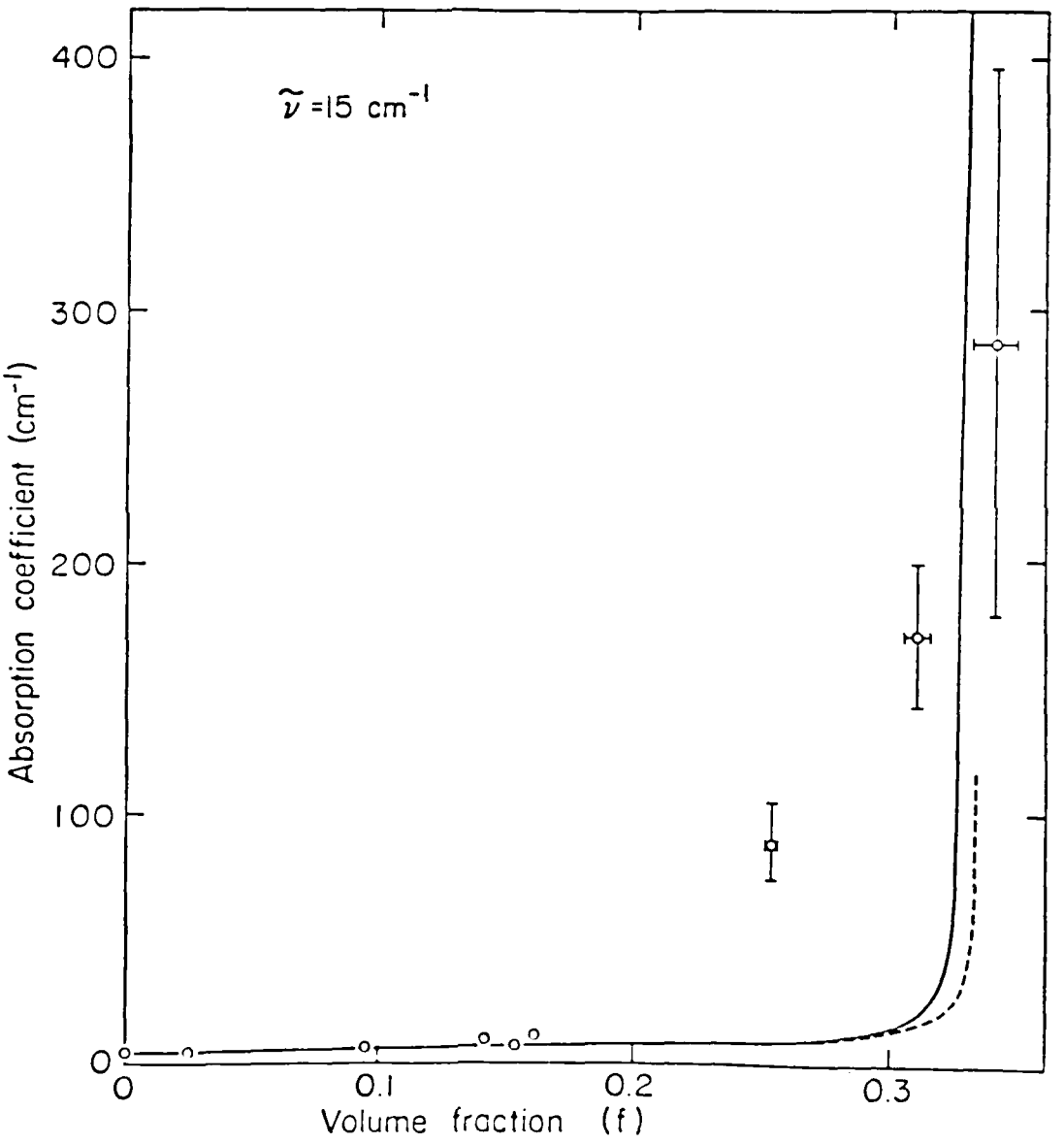

Figure 3. Volume fraction dependence of the far infrared absorption coefficient at $\tilde{\nu}$ = 15 cm^{-1} for Ag particles in gelatin. The circles indicate the data. The solid line shows the prediction of the Bruggeman model for 100Å diameter Drude Ag particles imbedded in gelatin. The dashed curve is the prediction of the Bruggeman model for particles made up of a perfect conductor.

REFERENCES

1. P.O. Nilsson, in Solid State Physics, H. Ehrenreich, F. Seitz, and D. Turnbull, eds. (Academic Press, New York 1974), Vol. 29, pp. 218-221.

2. M.L. Théye, Phys. Rev. B 2, 3060 (1970).

3. M.M. Dujardin and M.L. Théye, J. Phys. Chem. Solids 32, 2033 (1971).

4. J.N. Hodgson, J. Phys. Chem. Solids 29, 2175 (1968).

5. T.E. Faber, Introduction to the Theory of Liquid Metals, (Cambridge Univ. Press, 1972) p. 383.

6. W.H. Weber and S.L. McCarthy, Applied Phys. Letters 25, 396 (1974).

7. W.H. Weber and S.L. McCarthy, Phys. Rev. B 12, 5643 (1975).

8. Z. Schlesinger and A.J. Sievers, Appl. Phys. Letters 36, 409 (1980).

9. M.A. Ordal, L.L. Long, R.J. Bell, S.E. Bell, R.W. Alexander and C.A. Ward, Appl. Optics 22, 1099 (1983).

10. C.G. Granqvist, R.A. Buhrman, J. Wyns, and A.J. Sievers, Phys. Rev. Lett. 37, 625 (1976).

11. D. Pramanik, MS Thesis, Cornell University, 1978, MSC Report #4220.

12. G.L. Carr, R.L. Henry, N.E. Russell, J.C. Garland, and D.B. Tanner, Phys. Rev. B 24, 777 (1981).

13. E. Simanek, Phys. Rev. Lett. 38, 1161 (1977); R. Ruppin, Phys. Rev. B 19 1318 (1979); P.N. Sen and D.B. Tanner, Phys. Rev. B 26, 3582 (1982).

14. A.J. Glick and E.D. Yorke, Phys. Rev. B 18, 2490 (1978); E. Simanek, Solid State Commun. 37, 97 (1981); A.A. Lushnikov, V.V. Maksimenko, and A.J. Simonov, Sov. Phys. Solid State 20, 292 (1978).

15. G.L. Carr, J.C. Garland, D.B. Tanner, Phys. Rev. Lett. 50, 1607 (1983).

16. N.E. Russell, J.C. Garland, and D.B. Tanner, Phys. Rev. B 23, 632 (1981).

17. G.L. Carr, R.L. Henry, N.E. Russell, J.C. Garland, and D.B. Tanner, Phys. Rev. B 24, 777 (1981).

18. R.P. Devaty and A.J. Sievers, Phys. Rev. Letters 52, 1344 (1984).

19. W.A. Curtin, R. C. Spitzer, N. W. Ashcroft and A. J. Sievers, Phys. Rev. Letters (1985).

V. PUBLICATIONS (1984-1985)

Program and Abstracts

Forty-Fourth Annual Conference on Physical Electronics

A Topical Conference on the Physics and Chemistry of Surfaces and Interfaces

Sponsored by the American Physical Society
Division of Condensed Matter Physics
Division of Electron and Atomic Physics

Co-hosted by

AT&T Bell Laboratories

Princeton University

Kresge Auditorium - Frick Laboratory
Princeton, New Jersey 08544
18-20 June 1984

Infrared Surface Plasmon Interferometry on Clean Metal Surfaces, L. M. Hanssen, D. M. Riffe, and A. J. Sievers, Cornell University, Ithaca, New York, 14853.

An interference phenomenon has been discovered on clean metal surfaces which involves plane electromagnetic waves (PEW's) and infrared surface plasmons (IRSP's). The interference is demonstrated with a two beam interferometer of fixed optical path and variable frequency. The identification of the interference minimum gives the first direct measurement of the IRSP index of refraction and hence the infrared plasma frequency.

IRSP's are TM (p-polarized) inhomogeneous surface waves which propagate along a metal/vacuum interface at nearly the velocity of light. For good metallic conductors the infrared surface wave attenuation coefficient $\alpha_s = \omega^2\rho/4\pi c$ where ω is the frequency, ρ the d.c. resistivity and c the velocity of light. In the same limit the index of refraction of this mode is $n_s = 1 + \omega^2/2\omega_p^2$ where ω_p is the infrared plasma frequency.

Because the IRSP wavevector is greater than that of light we use gratings etched into a W(100) surface to couple CO_2 laser radiation to and from IRSP's. We find that these grating couplers not only excite the IRSP mode but also excite plane waves at the same frequency. These PEW's are produced in the form of a packet traveling in the forward direction and spreading slowly in width. The IRSP travels along the surface with a phase velocity c/n_s while the phase velocity of the PEW's which travel above the surface is c. At the output grating coupler which is a distance ℓ from the input grating the IRSP and PEW packet both contribute to the output amplitude; however, these two contributions are no longer in phase. The total intensity of the resultant PEW's launched by the second grating is

$$I = I_S + I_{PEW} + 2(I_S I_{PEW})^{\frac{1}{2}} \cos\theta$$

where $\theta = [(n_s - 1)\,\omega\ell/c + \phi]$ with ϕ a constant. Complete destructive interference occurs when $\theta = (2m + 1)\,\pi$ and $I_S = I_{PEW}$. For W(100) and a path length of 5 cm the phase is adjusted to destructive interference by varying the CO_2 laser frequency from 900 cm^{-1} to 1080 cm^{-1}. In order to obtain equal intensity in the two arms of the interferometer, the sample temperature is varied. Since $\rho \sim T$ and $I_S \sim \exp(-\alpha_s \ell)$, a modest temperature excursion changes this component by orders of magnitude. For W(100) the interference gives $\hbar\omega_p = 6.8$ eV. The addition of a monolayer of oxygen to the clean surface is observed to unbalance this optical bridge and produce an increase in the output signal of 4%.

The infrared surface plasmon interferometer can be realized for poor conductors as well as good ones such as W. If the surface propagation length, ℓ, is made long enough so that a π phase change can occur between the two optical paths, then for any conductor the condition for sufficient IRSP intensity at the output is simply $\alpha_s \ell = 2\pi/\omega\tau$ where τ is the electron relaxation time. Thus the interference can be observed as long as the infrared frequency is chosen such that $\omega\tau > 1$.

Work supported by NSF Grant No. DMR-81-06097 and by the Air Force under Grant No. AFOSR-81-0121B. Materials Science Center Report No. 5285.

Observation of an index-of-refraction-induced change in the Drude parameters of Ag films

H. Gugger,* M. Jurich, and J. D. Swalen
IBM Research Laboratory, San Jose, California 95193

A. J. Sievers
Laboratory of Atomic and Solid State Physics and Materials Science Center, Cornell University, Ithaca, New York 14853

(Received 29 December 1983; revised manuscript received 13 April 1984)

The method of attenuated total internal reflection has been used in the visible region to obtain precise values of the dielectric function of Ag films in contact with different dielectric media. By measuring, at eight visible laser wavelengths, the surface-plasmon resonance of an Ag film against air and then against an organic liquid, we show that for both cases the dielectric function can be described by the Drude model with the well-known frequency-dependent relaxation time, namely, $\tau^{-1}(\omega)=\tau_0^{-1}+\beta\omega^2$. The interesting results are that $\tau_0^{-1}(\text{liquid})>\tau_0^{-1}(\text{air})$, that $\beta(\text{liquid})<\beta(\text{air})$, and that the plasma frequency $\omega_p(\text{liquid})>\omega_p(\text{air})$. The fact that β changes—the sign of the change or its magnitude—appears to eliminate all previous models which have been proposed to describe this frequency-dependent term. The observed changes in β and ω_p are consistent with the idea of a complex relaxation time whose real and imaginary parts are connected in a causal way. The index-of-refraction dependence of the Drude parameters demonstrates that surface electrodynamics must play an important role. The observed trends reported here could be accounted for if increasing the index of the dielectric half-space would increase the attractive surface-plasmon interaction and decrease the magnitude of electron-electron scattering in the Ag surface.

I. INTRODUCTION

The optical data for the noble metals at frequencies below the interband absorption edge are accurately characterized by the free-electron Drude model.[1] The real and imaginary parts of the metal dielectric function can be written as

$$\epsilon_1 \simeq \epsilon_\infty - \frac{\omega_p^2}{\omega^2} \tag{1}$$

and

$$\epsilon_2 = \frac{\epsilon_\infty - \epsilon_1}{\omega\tau} \tag{2}$$

in the limit where $\omega\tau \gg 1$. The three parameters of the model are ϵ_∞, the core polarizability and interband contribution to the dc dielectric constant, $\omega_p^2 = 4\pi Ne^2/m$, the plasma frequency squared, and τ^{-1}, the electron scattering rate. For the noble metals, this scattering rate has the form[1]

$$\tau^{-1} = \tau_0^{-1} + \beta\omega^2 . \tag{3}$$

Both τ^{-1} and to a lesser extent ω_p are found to vary depending on the sample preparation techniques.[2,3] The source of these variations remains poorly understood.

Because annealing thin-film Au samples[2] decreases the size of β, an inhomogeneous medium model composed of crystalline grains and disordered intergranular material has been used with a two-carrier Drude model to account for the quadratic dependence of the relaxation time.[4] However, it is unlikely that the nonzero β observed for single-crystal bulk samples[5] also can be explained in this manner. The possibility that the frequency-dependent term stems from electron-electron scattering has been considered in some detail by Christy and co-workers.[6,7] They have not been able to obtain quantitative agreement with the electron-electron contribution inferred from the measured electrical and thermal resistivities. Recently, Smith and Ehrenreich[8] have proposed that this frequency dependence follows from a more precise estimate of the electron-phonon interaction. Their numerical estimate of the β's are in reasonable agreement with the room-temperature experimental values.

A consistent explanation of the variations observed for ω_p has not yet been found although the changes are usually assigned to surface morphology. The ω_p's measured for the thin semitransparent Au films investigated by Théye are about 5% larger than the values reported for electropolished bulk samples.[2] Almost the same change in ω_p has been measured by Hodgson for the internal and external surface of an opaque Au film[9] with the larger ω_p occurring for the film-substrate interface. By studying surface-plasmon resonance excitation at both surfaces of evaporated metal films, Weber and McCarthy confirmed the Au results and showed that a similar effect existed for Ag films.[10,11] They found that the ω_p at the substrate interface was consistently about 5% larger than ω_p at the air interface, independent of the growth rate of the film which was varied over a factor of 100. They also proposed that this difference could be understood if the Ag film density near the air surface was several percent below that near the substrate interface.

To date, both the relaxation rate and the plasma frequency of the noble metals have been treated as independent quantities, although in general, if τ depends on fre-

quency, so must ω_p.[12–15] This interrelation between the frequency dependences of the two Drude model parameters has been demonstrated in a detailed analysis of the phonon-assisted absorption process.[13] The two frequency-dependent Drude model parameters $\omega_p(\omega)$ and $\tau(\omega)$ are given by

$$[\omega_p(\omega)]^2=\frac{\omega_p^2}{1+\bar{\lambda}(\omega)} \tag{4}$$

and

$$\tau(\omega)=\bar{\tau}(\omega)[1+\bar{\lambda}(\omega)]\,, \tag{5}$$

where the frequency dependence of $\bar{\lambda}(\omega)$ is intimately related to the Kramers-Kronig transform of $[\omega\bar{\tau}(\omega)]^{-1}$.

One analysis of the infrared and optical properties of the alkali metals has been made[15] which makes use of expressions similar to Eqs. (4) and (5). An intrinsic surface-plasmon-assisted absorption process was proposed to account for the enhanced infrared mass. It is a Holstein-type process with the surface plasmons taking the role of the phonons. One of the predictions of the surface-plasmon-assisted absorption model is that both Drude parameters of the metal should depend on the dielectric constant of the neighboring substrate. Consequently, the observed variations in the optical properties of the noble-metal films could be a function of the index of refraction of the dielectric substrate as well as surface morphology. One purpose of this paper is to report on our experimental test of this possibility.

By using liquid dielectrics together with the surface-plasmon resonance technique, we have measured the change in the dielectric function of Ag films with a constant surface structure as a function of the interface dielectric constant. The previously reported change[10] in plasma frequency between Ag-glass and Ag-air interfaces is reproduced in our experiments. When liquids with various refractive indices are placed on the same surface where Ag-air measurements were made, β is observed to decrease consistent with a decrease in the mass parameter (an increase in ω_p).

The fact that β changes at all in our experiments is not compatible with the usual assignment to electron-electron[7] or electron-phonon[8] processes. In addition, mechanisms which rely on metal grains,[4] surface roughness, a reduced film density near the air interface,[11] or surface-plasmon-assisted absorption[15] cannot account for the observed increase in ω_p. However, the dielectric constant dependence of the experimental results demonstrates that the Drude model parameters are controlled by a surface process in which electrodynamics plays an important role. The sign of the effect is consistent with the dielectric reducing the first moment of the induced surface charge and hence reducing the size of the electron-hole excitation term, or with a dielectric enhanced surface-plasmon interaction reducing the magnitude of the surface electron-electron scattering term.

In the next section, the attenuated total internal reflection apparatus and experimental measurements are described. The Ag-air and Ag-liquid interface results are presented in Sec. III. We demonstrate in Sec. IV that the experimental data are consistent with the dielectric induced change in both the frequency-dependent scattering rate and the electron mass.

II. EXPERIMENTAL DETAILS

A. Attenuated total internal reflection (ATR) apparatus

We have used surface-plasmon resonance excitation at a number of laser wavelengths to determine the dielectric function of Ag in the visible regions.[16] The attenuated total reflection setup is shown in Fig. 1.

Reflectivity measurements were done with the prism mounted on a computer-controlled rotating table to scan the angle of incidence and collect the digitized data. The wavelengths used were from an argon-ion laser (488.0 and 514.5 nm), from a krypton-ion laser (530.9, 568.2, 647.1 and 676.4 nm), from a helium-neon laser (632.8 nm), and from a helium-cadmium laser (441.6 nm). To achieve better rejection of the light with the unwanted polarization, two Glan-Thompson prism polarizers were placed sequentially in front of a Fresnel rhomb.

Since the surface-plasmon resonance occurs exclusively upon excitation with TM waves, the correct angle of polarization was set by rotating the rhomb to a minimum reflection for TM light, i.e., at the angle of maximum plasmon absorption. The coated prism was positioned in such a way that the chopped laser beam always refracted to the center portion of the film to minimize beam walk. The reflected signal at twice the angle was detected with a p-i-n photodiode. A fraction of the chopped laser beam was split off before the prism with a pellicle beam splitter to serve as the laser intensity reference. Both signals, the reflection and the laser reference signal, were separately detected and amplified; their ratio gave the final output.

B. Procedure

The Ag films, approximately 500 Å thick, were vacuum deposited onto the base of LaSF31 Schott glass isosceles prisms at a rapid rate (50–100 Å/s) to obtain a fine grained surface. Prisms with apex angles of 53° or 57° were used so that the critical angle of the glass/air interface could be observed.

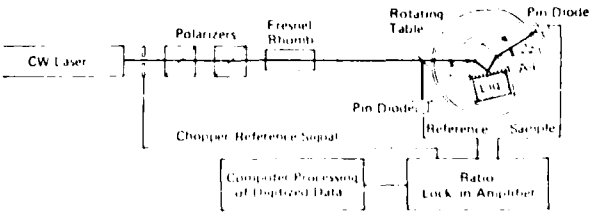

FIG. 1. Schematic diagram of experimental apparatus. A Teflon cup containing air or liquid was pressed with a split o-ring onto the silver film on the base of a high-refractive-index prism. Two Glan-Thompson prism polarizers were used to improve rejection of the other polarization. Rotation of the Fresnel rhomb allowed conversion between s and p polarizations. The rotating table included an arm at 2θ to track the reflected beam.

We measured the angles of each prism by differences in the angles of back reflection. Then we determined the refractive index of the prisms by comparing the results from different methods.

(1) The glass-melt information sheet[17] for our Schott glass (LaSF31) prisms gave the refractive index at selected wavelengths and constants for a power-series expansion of the dispersion curve. These data were then used to calculate the refractive indices at our laser wavelengths.

(2) From a measurement of a critical angle θ_c, the refractive index can be calculated from Snell's law.

(3) From the minimum angle of deviation measured for the prism and knowing the prism angle, the refractive index was calculated.[18]

Since all three values agreed within experimental error at all wavelengths, we decided to use the easily calculated values from the Schott data.

The prism angle was checked at each wavelength by the critical angle for the glass-air interface. Standard deviations for these determinations using eight wavelengths were typically $\pm 0.005°$. From the prism index and prism angle, the index of refraction of the liquid n could then be calculated from the experimentally observed change in critical angle θ_c when a liquid replaces air without any further experiments. Since n is a function of, e.g., wavelength, purity, and temperature, this procedure directly gave the index for our experimental conditions.

The first measurement for every freshly coated silver film was an ATR experiment at the silver-air interface to determine the dielectric constants of bare silver at all wavelengths under investigation, as well as the thickness of the film. This measurement was to identify any differences in the dielectric function of Ag that might arise from surface morphology. Then, carbon tetrachloride ($n \sim 1.46$) or hexane ($n \sim 1.37$) were placed next to the Ag and the dielectric constants at the Ag-liquid interface were determined. In Fig. 2, the angular location of the critical angle is shown for a typical ATR curve at a silver-hexane interface, with the critical angle being essentially that for hexane-glass.

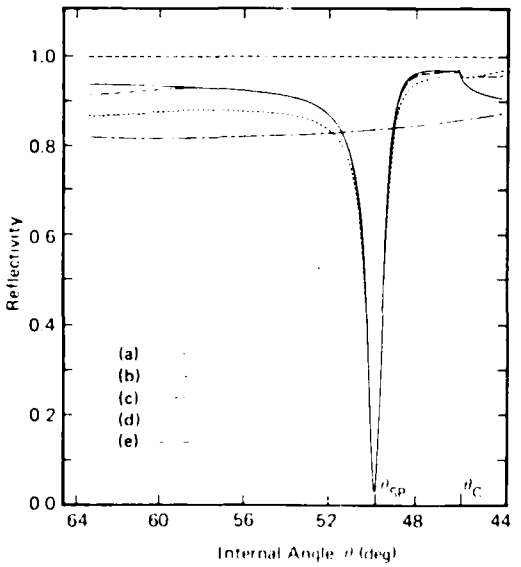

FIG. 2. Typical reflectivity curve as a function angle. For this example, hexane is adjacent to Ag. θ_{SP} is the reflectivity minimum at the surface-plasmon angle and θ_c is the critical angle of air or liquid and the prism. Curves: (a) experimental curve; (b) prism absorption loss; (c) prism reflection loss from both faces; (d) experimental curve corrected for absorption, reflections, and background; (e) calculated "best fit" of the Fresnel equations.

III. RESULTS

The values of the complex dielectric function of Ag were calculated by a least-squares fit of the exact Fresnel reflection formulas to the experimental ATR curves. The matrix procedure outlined by Heavens[19] was used to calculate the reflectivity for a layered structure. From the experimental reflectivity curves for the Ag-air interface, we determined ϵ_1 and ϵ_2 for each wavelength and the thickness of the film. When the liquid was introduced, we again used a least-squares-fitting procedure to obtain ϵ_1 and ϵ_2, but now the thickness of the Ag film was set equal to the average value determined for the Ag-air-interface measurement. The measured values for the films are listed in Table I.

Initially, the calculated reflectivity curves deviated significantly from the experimental ones. Searching for sources of this deviation, it was determined that at least four factors contribute: (1) reflection losses at each face of the prism, (2) absorption from transmission through the prism, especially at short wavelengths, (3) movement of the beam from one section to another section of the film with slightly different optical properties as the prism is rotated, and (4) dark current of the measurement system. In order to correct for these deviations, we collected both TE and TM ATR data from which we subtracted

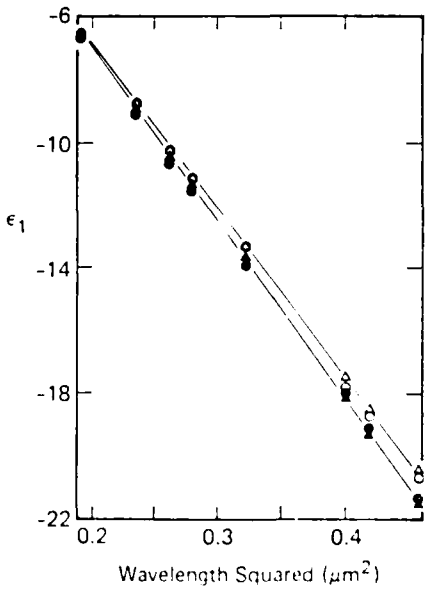

FIG. 3. Measured real part of the dielectric function of silver versus wavelength squared for both air △ and CCl_4 ▲ half-spaces and air ○ and hexane ● half-spaces. The lines are average values and given to clearly show the trends.

TABLE I. Experimentally determined dielectric function of Ag and related optical parameters. (Straight line shown in Fig. 4 without the point of 4416 Å because it is more than three standard deviations from the line.)

	Liquid			Air		
λ (Å)	ϵ_1	ϵ_2	τ_e^{-1} (10^{14} s^{-1})	ϵ_1	ϵ_2	τ_e^{-1} (10^{14} s^{-1})
CCl_4			$d=58.4\pm0.4$ nm			
4416	−6.471	0.4191	1.634	−6.323	0.4755	1.953
4880	−9.087	0.5139	1.463	−8.772	0.5243	1.577
5145	−10.528	0.6239	1.523	−10.265	0.6074	1.552
5309	−11.486	0.6547	1.456	−11.150	0.6387	1.490
5682	−13.834	0.7855	1.423	−13.374	0.7003	1.332
6328	−17.940	1.0091	1.340	−17.452	0.9599	1.329
6571	−19.334	1.0537	1.289	−18.582	0.9473	1.218
6764	−21.448	1.2074	1.298	−20.487	1.0270	1.165
Hexane			$d=37.4\pm0.1$ nm			
4416	−6.6037	0.4464	1.761	−6.567	0.3549	1.416
4880	−9.122	0.4739	1.3721	−8.749	0.4098	1.229
5145	−10.606	0.5452	1.347	−10.230	0.4524	1.154
5309	−11.609	0.5752	1.290	−11.155	0.4785	1.111
5682	−13.922	0.6808	1.245	−13.385	0.5570	1.055
6328	−18.129	0.9657	1.287	−17.772	0.7140	0.971
6471	−19.133	0.9513	1.187	−18.701	0.7492	0.956
6764	−21.409	1.0408	1.132	−20.650	0.8073	0.908

the dark current from each. In the prism, absorption losses were very small because of the relatively long wavelength and good transmission quality of the high-index glass. Hence we used the measured TE data to calculate a correction curve for absorption losses after correcting for its reflection losses. These absorption corrections including those for TM reflection losses were then applied to the TM curves. The various reflectivity and correction curves are shown in Fig. 2. Note the close agreement between the corrected experimental curve and the calculated curve, indicating the precision with which the values of the dielectric function given in Table I describe the experimental measurements.

In Fig. 3 we plot our experimental values for the real part of the dielectric function of silver versus wavelength squared for both the air-silver and liquid-silver cases. Two different liquids have been studied, CCl_4 and hexane. The values for $\omega_{p,e}^2$ and ϵ_∞ were obtained from a least-squares fit to an ϵ_1-versus-λ^2 line for both the Ag-air and Ag-liquid data. These derived experimental numbers are recorded in Table II.

The inverse relaxation time from the experimental values for ϵ_1 and ϵ_2 at each frequency is obtained from

$$\tau_e^{-1}=\frac{\omega\epsilon_2}{\epsilon_\infty-\epsilon_1}\ . \tag{6}$$

Figures 4(a) and 4(b) show a plot of τ_e^{-1} versus ω^2 for Ag in contact with CCl_4 and hexane, respectively. To a good approximation, these data can be fitted by Eq. (3). The values of τ_0^{-1} and β obtained from a least-squares fit to these data are given in Table II.

IV. DISCUSSION

The experimental results clearly show that the effective dielectric function of the metal is changed when liquid replaces air. Could these results be explained by surface roughness on the Ag film? A metal-insulator composite layer is often used to model the optical properties of a roughened surface.[10,20] According to the Maxwell-Garnett theory, a Lorenz-Lorentz type of dispersion will occur in such a layer. We find that replacing a 100-Å-

TABLE II. Experimentally determined Ag Drude model parameters.

	Film no. 1		Film no. 2	
	Air	CCl_4	Air	Hexane
ϵ_∞	4.07±0.08	4.47±0.11	4.14±0.08	4.22±0.06
$\omega_{p,e}^2$ (eV)	9.10±0.02	9.33±0.03	9.14±0.02	9.27±0.02
τ_0^{-1}(10^{13} s^{-1})	6.4 ±0.9	10.5 ±0.5	5.5 ±0.5	9.61±0.32
β_0 [10^{12} $s^{-1}(eV)^{-2}$]	16.1 ±1	7 ±2	11 ±1	6 ±1
λ_0 (10^{-2})	9.8 ±3	4.5 ±1.4	7.5 ±2.4	4.5 ±1.4
α^{-1} (eV)	9 ±4	9 ±4	11 ±4	11 ±4
ω_p (eV)	9.5 ±0.1	9.5 ±0.1	9.5 ±0.1	9.5 ±0.1

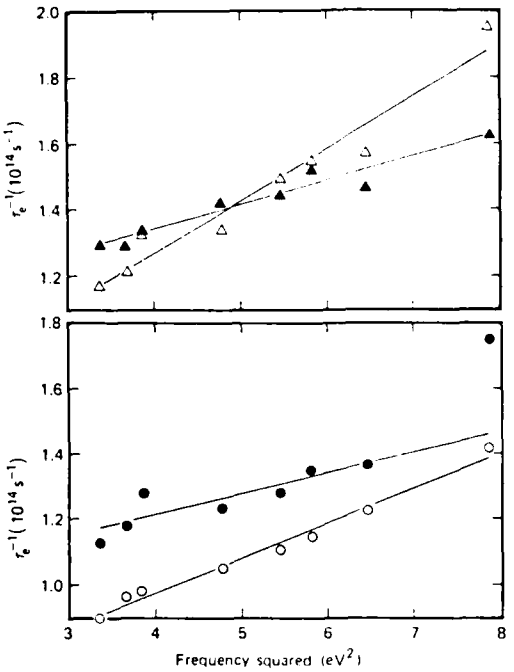

FIG. 4. Relaxation time calculated from the measured values of dielectric function of silver with Eq. (6), as a function of energy squared: (a) air △, CCl_4 ▲, and (b) air ○, hexane ●.

thick composite Ag-air layer on a silver film with a Ag-liquid composite layer of the same thickness causes the predicted ATR minimum at the Ag-liquid interface to shift to increasing internal angles corresponding to a less negative real part of the dielectric function. (Our measured shift is always to *decreasing* internal angles with respect to the predicted ATR minimum at the Ag-liquid interface from the Ag-air data.) Hence, although it is possible to account for the air-Ag results by adjusting the parameters in the Maxwell-Garnett model, once these parameters are fixed, the model cannot account for the liquid-Ag data. Inspection of the data in Fig. 3 and Table I shows that for both films a composite medium layer would be expected to produce the opposite effect on the real part of the dielectric function to what is observed experimentally. In addition, Maxwell-Garnett theory implies that the largest influence should be at short wavelengths close the sphere resonance condition, but experimentally the largest percentage change in ϵ_1 is observed in the long-wavelength region.

Another possibility is the two-carrier model for crystallites (a) and grain boundaries (b) proposed by Nagel and Schnatterly.[4] For the limit $\omega\tau_a > 1$, $\omega\tau_b \ll 1$, and $(2N_b/N_a)\ \omega^2\tau_b^2 \ll 1$, they find an effective relaxation time which is frequency dependent, namely,

$$\tau^{-1} = \tau_a^{-1} + \frac{N_b}{N_a}\tau_b\omega^2 . \tag{7}$$

In this expression, τ_a is due to scattering from phonons in crystallites while τ_b is very much smaller and is presumably controlled by the thickness of the grain boundaries. N_b/N_a is the ratio of the average grain size to the average crystallite size.

In Table II it is seen that the frequency-independent contribution (τ_0^{-1}) to the relaxation time increases by about a factor of 2 when air is replaced by a liquid. The mechanical modulation of the metal surface by the thermal fluctuations in the liquid could account for this observation; hence in Eq. (7) an increase in τ_a^{-1} is to be expected. Since τ_b^{-1} is already larger than the optical probing frequency, the thermal fluctuations in the liquid should not have much effect on the grain-boundary relaxation times, certainly nothing like the factor of 2 observed for β of Table II. On these grounds, the two-carrier model can be eliminated as the source of the frequency-dependent relaxation time.

The change in β observed for the air-liquid substitution is not compatible with relaxation mechanisms which rely solely on bulk processes. Identification with the usual electron-electron or electron-phonon scattering now seems unlikely.

We now demonstrate that the measured change in the optical constants are consistent with a dielectric induced change both in the electron frequency-dependent scattering rate and in the optical mass. If we define the complex frequency-dependent electron scattering rate as

$$\hat{\tau}^{-1} = \hat{\Gamma} = \Gamma_1 + i\Gamma_2 , \tag{8}$$

and for later convenience set $\Gamma_2 \equiv -\omega\lambda$, then the Drude expressions become

$$\epsilon_\infty - \epsilon_1(\omega) = \frac{\omega_p^2}{\Gamma_1^2}(1+\lambda)\left[\left[\frac{\omega}{\Gamma_1}\right]^2(1+\lambda)^2+1\right]^{-1} \tag{9}$$

and

$$\epsilon_2(\omega) = \frac{\omega_p^2}{\omega\Gamma_1}\left[\left[\frac{\omega}{\Gamma_1}\right]^2(1+\lambda)^2+1\right]^{-1} . \tag{10}$$

The experimental relaxation frequency is

$$\tau_e^{-1} = \frac{\omega\epsilon_2(\omega)}{\epsilon_\infty - \epsilon_1(\omega)} = \Gamma_1(1+\lambda)^{-1} \tag{11}$$

and the experimental plasma frequency squared is

$$\omega_{p,e}^2 \approx \omega^2[\epsilon_\infty - \epsilon_1(\omega)] = \omega_p^2(1+\lambda)^{-1} . \tag{12}$$

The quadratic frequency dependence observed for the electron scattering rate in noble metals can be modeled if $\hat{\Gamma}$ is taken to have the following approximate causal form:

$$\Gamma_1 = \Gamma_d + \lambda_0\omega^2\alpha(1+\omega^2\alpha^2)^{-1} \tag{13}$$

and

$$\lambda = \lambda_0(1+\omega^2\alpha^2)^{-1} . \tag{14}$$

Then

$$\Gamma_1 = \Gamma_d + \beta\omega^2 , \tag{15}$$

where

$$\beta = \alpha\lambda . \tag{16}$$

In the limit that $\lambda \ll 1$, Eq. (11) shows that Γ_1 is a good approximation to τ_e^{-1}. For the limit $\alpha\omega \ll 1$ which we

sume in the analysis of the data below $\lambda \rightarrow \lambda_0$ and $\beta \rightarrow \beta_0$, so both parameters are frequency independent and the real part of the relaxation rate contains a pure quadratic term.

The second assumption which we introduce is that α is independent of the presence of the dielectric half-space. This assumption is reasonable since even if α^{-1} is related to the electrostatic surface-plasmon mode frequency in Ag, this mode is pinned at a fixed frequency, by the high-frequency interband transitions, independent of the dielectric index of refraction.

The subscripts l and a are used to distinguish between the measured Ag-liquid and Ag-air interface results. From Eq. (16)

$$\frac{\beta_{a0}}{\beta_{l0}} = \frac{\lambda_{a0}}{\lambda_{l0}} \tag{17}$$

and from Eq. (12)

$$\frac{(\omega_{p,e}^2)_l}{(\omega_{p,e}^2)_a} = \frac{1+\lambda_{a0}}{1+\lambda_{l0}} . \tag{18}$$

These two experimental numbers enable us to determine both λ_{a0} and λ_{l0} which are presented in Table II for both films. The measured value for β_{a0} is then used to estimate α^{-1}. This parameter value which is consistent with the $\omega\alpha \ll 1$ assumption is remarkably close to the value of the Ag plasma frequency.

A consistent set of parameters λ_{a0}, λ_{l0}, and α^{-1} is found which describes the frequency-dependent relaxation time represented by Eqs. (13) and (14). The good agreement between experiment and this phenomenological model over the visible region demonstrates that the change in the optical properties is due to a dielectric induced change in the electron relaxation time. Somewhat surprising is the sign of the change.

For the alkali metals it has been shown that a surface-plasmon-assisted photon absorption mechanism[15] which leads to an initial ω^4 dependence of the Drude scattering rate is consistent with the experimental data if the magnitude of the mechanism is used as a free parameter. It was also shown that increasing the index of refraction of the neighboring dielectric half-space increases the strength of this term, increases λ, and hence *decreases* ω_p. The fact that the optical properties of the noble metals change in the opposite way when the index of refraction is increased is a clear indication that this mechanism cannot be the dominant factor here.

It has been known for some time that when a metal surface is probed with TM polarized radiation, electron-hole (e-h) pair excitation should contribute to the optical absorption.[21–23] Recently, Ljungbert and Apell[24] have proposed that this effect can be described in terms of a single parameter, the first moment of the induced surface charge of the metal. From their calculation of the relative contribution of electron-hole pairs to the total absorptance, we can estimate the magnitude of the appropriate frequency-dependent scattering rate which describes this process. For $\omega \ll \omega_p$ we find[24]

$$\gamma_a^{\prime} \simeq \frac{\omega^2}{c} |\mathrm{Re}\, d_\perp(0)| , \tag{19}$$

where $|\mathrm{Re}\, d_\perp(0)|$ is the center of gravity of the induced charge which is measured with respect to the edge of the positive metal background. Although the magnitude of this relaxation term is estimated from Ref. 24 to be less than 4% of the strength needed to explain the data in Table II, it does have the correct frequency dependence. Moreover, because of the Pauli exclusion principle, the quantity $|\mathrm{Re}\, d_\perp(0)|$ for a liquid-metal interface should be smaller than $|\mathrm{Re}\, d_\perp(0)|$ for an air-metal interface. It is not clear to us, though, how this parameter could change by the measured factor of 2 observed for β (see Table II).

The large change in β required for the electron-hole excitation mechanism leads us to speculate on another possibility which again makes use of surface plasmons but now in an indirect role. The fact that the optical properties of the alkali metals and noble metals seem to change in opposite ways when the index of refraction of the half-space changes may be simply an indication of the size of the electron-electron scattering term within the skin depth of each metal type. Inkson[25] has pointed out that although the surface-plasmon interaction itself is attractive below the electrostatic mode limit, the decrease in the bulk-plasmon exchange interaction near the surface causes the total interaction for quasiparticles to be more repulsive than in the bulk.

If, below the electrostatic mode frequency, electron-electron scattering dominates the surface-plasmon-mediated scattering within a skin depth for the noble metals while the converse is true for the alkali metals, then a consistent picture emerges. Increasing the index of the dielectric half-space would increase the strength of the attractive surface-plasmon interaction for both metal types and decrease the magnitude of the electron-electron scattering term within a skin depth, but this decrease would only be apparent in the optical properties of the noble metals.

Although it has been known for many years that the Drude parameters of noble-metal films depend on surface morphology and many relaxation processes have been invoked to explain the quadratic frequency dependence of the electron relaxation frequency, it was not generally recognized that surface electrodynamics could play an important role at such low frequencies. Our systematic study of an index-of-refraction induced change in the Drude parameters of Ag films demonstrates that this is the case. More experiments need to be carried out to identify the physical process, but the general conclusion is now clear: The dielectric function required to describe the ir and optical properties of a noble-metal mirror depends on the dielectric constant of the adjoining medium.

ACKNOWLEDGMENTS

One of us (H.G.) acknowledges support by IBM. The initial work by A. J. Sievers was supported by the NSF under the Visiting Scientist program. Continuing support has been obtained from the National Science Foundation under Grant No. DMR-81-[illegible] and from U.S. Air Force Office of Scientific Research under Grant No. AFOSR-81-0121.

*Permanent address: Ciba-Geigy AG, KA Forschungszentrum, CH-1701 Fribourg, Switzerland.

[1]P. O. Nilsson, in *Solid State Physics*, edited by H. Ehrenreich, F. Seitz, and D. Turnbull (Academic, New York, 1974), Vol. 29, pp. 218–221.

[2]M. L. Theye, Phys. Rev. B **2**, 3060 (1970).

[3]M. M. Dujardin and M. L. Théye, J. Phys. Chem. Solids **32**, 2033 (1971).

[4]S. R. Nagel and S. E. Schnatterly, Phys. Rev. B **9**, 1299 (1974).

[5]S. Roberts, Phys. Rev. **118**, 1509 (1960).

[6]R. T. Beach and R. W. Christy, Phys. Rev. B **16**, 5277 (1977).

[7]G. R. Parkins, W. E. Lawrence, and R. W. Christy, Phys. Rev. B **23**, 6408 (1981).

[8]J. B. Smith and H. Ehrenreich, Phys. Rev. B **25**, 923 (1982).

[9]J. N. Hodgson, J. Phys. Chem. Solids **29**, 2175 (1968).

[10]W. H. Weber and S. L. McCarthy, Appl. Phys. Lett. **25**, 396 (1974).

[11]W. H. Weber and S. L. McCarthy, Phys. Rev. B **12**, 5643 (1975).

[12]T. Holstein, Ann. Phys. (N.Y.) **29**, 410 (1964).

[13]P. B. Allen, Phys. Rev. B **3**, 305 (1971).

[14]J. W. Allen and J. C. Mikkelsen, Phys. Rev. B **15**, 2952 (1977).

[15]A. J. Sievers, Phys. Rev. B **22**, 1600 (1980).

[16]I. Pockrand, Surf. Sci. **72**, 577 (1978).

[17]Schott Glass Co. (private communication).

[18]M. Born and E. Wolf, *Principles of Optics* (Pergamon, Oxford, 1980), pp. 177–181.

[19]O. S. Heavens, *Optical Properties of Thin Solid Films* (Dover, New York, 1965), pp. 69–74.

[20]G. J. Kovacs, in *Electromagnetic Surface Modes*, edited by A. D. Boardman (Wiley, New York, 1982), p. 143.

[21]P. J. Feibelman, Phys. Rev. B **14**, 762 (1976).

[22]K. L. Kliewer, Phys. Rev. B **14**, 1412 (1976).

[23]P. J. Feibelman, Prog. Surf. Sci. **12**, 287 (1983).

[24]A. Ljungbert and P. Apell, Solid State Commun. **46**, 47 (1983).

[25]J. C. Inkson, J. Vac. Sci. Technol. **11**, 943 (1974).

Mie resonance for spherical metal particles in an anisotropic dielectric

R. P. Devaty
Naval Research Laboratory, Washington, D.C. 20375

A. J. Sievers
Laboratory of Atomic and Solid State Physics and Materials Science Center, Cornell University, Ithaca, New York 14853

(Received 20 August 1984)

The absorption coefficient for small metal particles randomly distributed in a uniaxial dielectric host is calculated using the Maxwell-Garnett effective-medium theory. Explicit expressions for the absorption coefficient are given for the limit of low metallic volume fraction. Incorporation of dielectric anisotropy into the theory provides improved agreement with published data on colloidal Na in NaN_3.

I. INTRODUCTION

A comparison of the frequency for maximum absorption ω_0 and line shape of the sphere resonance as predicted by the classical Mie theory[1] with data on small metal particles supported in dielectric hosts reveals systematic discrepancies. For example, there is a red shift of the measured value of ω_0 with respect to Mie theory for alkali-metal particles in colored alkali halides.[2]

The dependence of ω_0 on the dielectric constant of the host might provide evidence to support or refute at least one proposed explanation[3] for the red shift. Unfortunately, it is very difficult to produce particles with the same properties (size, distribution, shape, etc.) reproducibly in a number of hosts, or even to determine the properties of the particles in a given sample.

An anisotropic dielectric in effect has more than one dielectric constant. A sample of spherical metal particles embedded in an anisotropic dielectric can be probed by electromagnetic waves of suitably chosen polarization and direction of propagation to accurately measure the dependence of ω_0 on the dielectric constant of the host.

The purpose of this paper is to discuss the absorption coefficient of a collection of small spherical metal particles randomly embedded in a uniaxial dielectric host using the Maxwell-Garnett[4] effective-medium theory. Explicit expressions for the absorption coefficient are given for the limit of small metal volume fraction f, for which the Mie theory applies. The specialization to the uniaxial case retains the important physics, simplifies the mathematics, and applies to the example, colloidal Na in sodium azide (NaN_3), chosen to illustrate the effect. For Na in NaN_3 the relative splitting predicted by the theory is less than 1% of ω_0.

This paper is organized as follows: Section II briefly reviews the physics of electromagnetic waves propagating in a transparent anisotropic dielectric. Section III derives the Maxwell-Garnett effective dielectric function for small metal spheres embedded in a uniaxial dielectric host. Section IV derives the absorption coefficient for both ordinary and extraordinary waves propagating in this uniaxial effective medium and presents explicit results for the low-f limit. Finally, Sec. V applies the theory to colloidal Na in NaN_3 and compares the results with the experimental data of Smithard.[5]

II. ELECTROMAGNETIC WAVES IN A UNIAXIAL DIELECTRIC

Landau and Lifshitz and Born and Wolf,[6,7] among others, discuss the propagation of electromagnetic waves in a *uniaxial* nonabsorbing dielectric crystal. The symmetric dielectric tensor can be diagonalized to yield the eigenvalues ϵ_x, ϵ_y, and ϵ_z along the principal axes. Let the z axis be the axis of symmetry for the uniaxial crystal. Then $\epsilon_x = \epsilon_y \equiv \epsilon_\perp$ and $\epsilon_z \equiv \epsilon_\parallel$. If $\epsilon_\parallel > \epsilon_\perp$ the crystal is called "positive." For plane waves Maxwell's equations require that the triplets **D**, **H**, and the wave vector **k** and **E**, **H**, and the Poynting vector **S** be mutually perpendicular. Therefore, **E**, **D**, **k**, and **S** are coplanar. **S** specifies the direction of energy propagation, which determines where the light actually goes. For a direction denoted by either **k** or **S**, two linearly polarized waves propagate in the crystal. The "ordinary" wave behaves just like a wave in an isotropic medium (**k**∥**S**, etc.). For the "extraordinary" wave, **S** is not parallel to **k** except for special directions. For example, both waves are ordinary for propagation parallel to the axis of symmetry. This degeneracy permits elliptically polarized waves as solutions.

A beam of light incident on a uniaxial crystal undergoes double refraction—there are two refracted beams. The Poynting vector of the extraordinary refracted wave need not lie in the plane of incidence.

Born and Wolf discuss propagation of light[8] in an absorbing uniaxial crystal in the limit of weak absorption, since the general problem is mathematically tedious. The dielectric tensor is now complex, but otherwise the derivation resembles that for the transparent dielectric. The solutions are elliptically polarized and **D** is not perpendicular to **k**.

III. THE EFFECTIVE DIELECTRIC FUNCTION

Consider the propagation of electromagnetic waves of wavelength λ in a medium of small spherical metal particles of radius a and complex dielectric function $\hat{\epsilon}=\epsilon'+i\epsilon''$ distributed randomly in a transparent uniaxial dielectric host characterized by the diagonal elements $\epsilon_x=\epsilon_y\equiv\epsilon_\perp$ and $\epsilon_z\equiv\epsilon_\parallel$ in the principal coordinate system. In the quasistatic limit, $\lambda\gg a$, the response of the medium can be described by an effective dielectric tensor $\bar{\epsilon}_{ij}(\omega)$. Let E_i be the component of $\mathbf{E}$ parallel to the ith principal axis of the host. The Maxwell-Garnett[4] effective dielectric function follows from a volume average of the electric field and electric displacement vectors, given by

$$\begin{aligned}\bar{E}_i &= fE_i^{(i)}+(1-f)E_i^{(e)}\ ,\\ \bar{D}_i &= \bar{\epsilon}_i\bar{E}_i = f\hat{\epsilon}E_i^{(i)}+(1-f)\epsilon_i E_i^{(e)}\ ,\end{aligned} \tag{1}$$

where $E_i^{(i)}$ and $E_i^{(e)}$ are the ith components of the electric fields inside and external to the metal particle, respectively, and f is the volume fraction of metal in the medium. Also required is the electrostatic boundary condition[9]

$$E_i^{(i)}=\frac{\epsilon_i}{\epsilon_i-L_i(\epsilon_i-\hat{\epsilon})}E_i^{(e)}\ . \tag{2}$$

The depolarization factor is[9]

$$L_i=\frac{a^3}{2(\epsilon_\perp^2\epsilon_\parallel)^{1/2}}\int_0^\infty\frac{ds}{(s^2+a^2/\epsilon_i)R_s}\ , \tag{3}$$

where

$$R_s^2=(s+a^2/\epsilon_\perp)^2(s+a^2/\epsilon_\parallel)\ . \tag{4}$$

The integrals can be evaluated.[9] According to Landau and Lifshitz,

$$L_\parallel=\begin{cases}\dfrac{1-e^2}{2e^3}\left(\ln\left|\dfrac{1+e}{1-e}\right|-2e\right), & \epsilon_\parallel<\epsilon_\perp\\ \dfrac{1+e^2}{e^3}(e-\tan^{-1}e), & \epsilon_\parallel>\epsilon_\perp,\end{cases} \tag{5}$$

$$L_\perp=(1-L_\parallel)/2\ ,$$

where

$$e=|(\epsilon_\parallel/\epsilon_\perp)-1|^{1/2}\ . \tag{6}$$

The field-matching condition in Eq. (2) is identical to that for an ellipsoidal particle in an isotropic dielectric,[10] for which the depolarization factors are determined by the shape of the ellipsoid. The Maxwell-Garnett effective dielectric tensor in the principal coordinate system, obtained by combining Eqs. (1) and (2), is

$$\bar{\epsilon}_i=\epsilon_i\frac{\{[\epsilon_i-L_i(\epsilon_i-\hat{\epsilon})]-f(1-L_i)(\epsilon_i-\hat{\epsilon})\}}{[\epsilon_i-L_i(\epsilon_i-\hat{\epsilon})]+fL_i(\epsilon_i-\hat{\epsilon})}\ . \tag{7}$$

The complex effective dielectric function retains uniaxial symmetry, so that $\bar{\epsilon}_x=\bar{\epsilon}_y=\bar{\epsilon}_\perp$ and $\bar{\epsilon}_z=\bar{\epsilon}_\parallel$.

For a plane wave of wave vector $\mathbf{k}$ (direction $\hat{k}$) propagating in the effective medium, manipulation of Maxwell's equations and the constitutive relation yields

$$(\bar{n}^2-\bar{\epsilon}_\perp)[\bar{n}^2\bar{\epsilon}_\perp(1-\hat{k}_z^2)+\bar{n}^2\bar{\epsilon}_\parallel\hat{k}_z^2-\bar{\epsilon}_\parallel\bar{\epsilon}_\perp]=0\ , \tag{8}$$

where $\bar{n}^2=\bar{\epsilon}=\bar{\epsilon}'+i\bar{\epsilon}''$. The roots of Eq. (8) are

$$\begin{aligned}\bar{\epsilon}_o &= \bar{\epsilon}_\perp\ ,\\ \bar{\epsilon}_e &= \frac{\bar{\epsilon}_\perp\bar{\epsilon}_\parallel}{\bar{\epsilon}_\perp(1-\hat{k}_z^2)+\bar{\epsilon}_\parallel\hat{k}_z^2}\ ,\end{aligned} \tag{9}$$

for the ordinary and extraordinary waves, respectively. Let θ be the angle between $\hat{k}$ and the z axis. For the extraordinary wave,

$$\begin{aligned}\bar{\epsilon}_e' &= \frac{\bar{\epsilon}_\perp'(\bar{\epsilon}_\perp'^2+\bar{\epsilon}_\perp''^2)\cos^2\theta+\bar{\epsilon}_\parallel'(\bar{\epsilon}_\perp'^2+\bar{\epsilon}_\perp''^2)\sin^2\theta}{(\bar{\epsilon}_\parallel'\cos^2\theta+\bar{\epsilon}_\perp'\sin^2\theta)^2+(\bar{\epsilon}_\parallel''\cos^2\theta+\bar{\epsilon}_\perp''\sin^2\theta)^2}\ ,\\ \bar{\epsilon}_e'' &= \frac{\bar{\epsilon}_\perp''(\bar{\epsilon}_\perp'^2+\bar{\epsilon}_\perp''^2)\cos^2\theta+\bar{\epsilon}_\parallel''(\bar{\epsilon}_\perp'^2+\bar{\epsilon}_\perp''^2)\sin^2\theta}{(\bar{\epsilon}_\parallel'\cos^2\theta+\bar{\epsilon}_\perp'\sin^2\theta)^2+(\bar{\epsilon}_\parallel''\cos^2\theta+\bar{\epsilon}_\perp''\sin^2\theta)^2}\ .\end{aligned} \tag{10}$$

IV. THE ABSORPTION COEFFICIENT

The problem has been reduced to a calculation of the absorption coefficient of a homogeneous absorbing anisotropic medium. For the ordinary wave,

$$\alpha_o=\frac{\omega}{c}(2|\bar{\epsilon}_o|-2\bar{\epsilon}_o')^{1/2}\ . \tag{11}$$

If $f\ll1$,

$$\alpha_o=\frac{f\omega\epsilon_1^{3/2}}{c}\frac{\epsilon''}{[\epsilon_1-L_1(\epsilon_1-\epsilon')]^2+L_1^2\epsilon''^2}\ . \tag{12}$$

For Drude-metal particles with bulk plasma frequency ω_p and high-frequency dielectric constant ϵ_∞, the frequency of the sphere resonance is approximately

$$\omega_\perp=\omega_p/[\epsilon_\infty+(L_\perp^{-1}-1)\epsilon_\perp]^{1/2}\ . \tag{13}$$

The ordinary wave lives up to its name. For the extraordinary wave,

$$\alpha_e=\frac{\omega}{c}(2|\bar{\epsilon}_e|-2\bar{\epsilon}_e')^{1/2}\ , \tag{14}$$

which is a complicated expression when written explicitly. In the Mie limit ($f\ll1$),

$$\begin{aligned}\alpha_e=\frac{f\omega}{c}&\frac{(\epsilon_\perp\epsilon_\parallel)^{3/2}\epsilon''}{[\epsilon_\parallel\cos^2\theta+\epsilon_\perp\sin^2\theta]^{3/2}}\\ &\times\left\{\frac{\cos^2\theta}{[\epsilon_\perp-L_\perp(\epsilon_\perp-\epsilon')]^2+L_\perp^2\epsilon''^2}\right.\\ &\left.+\frac{\sin^2\theta}{[\epsilon_\parallel-L_\parallel(\epsilon_\parallel-\epsilon')]^2+L_\parallel^2\epsilon''^2}\right\}.\end{aligned} \tag{15}$$

This result can also be obtained by following Born and Wolf's[8] procedure for the limit of weak absorption. For Drude-metal particles, unless $\theta=0$ or $\pi/2$, there are two resonance frequencies, $\omega_\perp$ [Equation (13)] and

$$\omega_\parallel=\omega_p/[\epsilon_\infty+(L_\parallel^{-1}-1)\epsilon_\parallel]^{1/2}\ . \tag{16}$$

The relative strength of the resonances depends on θ. If

$\epsilon_\perp = \epsilon_\parallel$, Eq. (15) reduces correctly to the familiar Mie expression for particles in an isotropic medium.

V. DISCUSSION

To measure the dependence of ω_0 on the dielectric constant of the host using small metal particles in a uniaxial dielectric, the ideal orientation of the sample is with the axis of symmetry in the plane of the surface. Then a linearly polarized wave at normal incidence could be coupled completely into the ordinary ($\omega_0 = \omega_\perp$) or extraordinary ($\omega_0 = \omega_\parallel$) wave in turn by rotating the plane of polarization. Since the composite medium absorbs radiation, the solutions are elliptically polarized, but the polarization is nearly linear in the limit of weak absorption.

An example of the system under consideration for which the sphere plasma resonance has been studied experimentally[5] is colloidal Na in colored NaN_3. NaN_3 is a rhombohedral crystal with $n_o = \sqrt{\epsilon_\perp} = 1.38$ and $n_e = \sqrt{\epsilon_\parallel} = 1.52$.[11] Smithard and Tran[12] performed a fit of the Drude model to the data of Smith[13] for ϵ' of Na to obtain $\hbar\omega_p = 5.54$ eV, and $\epsilon_\infty = 1.25$. For these values, Eqs. (5), (6), (13), and (16) give $\varrho = 0.462$, $L_\perp = 0.320$, $L_\parallel = 0.359$, $\hbar\omega_\perp = 2.41$ eV (5148 Å), and $\hbar\omega_\parallel = 2.39$ eV (5185 Å). The splitting is less than 1% of the resonance frequency, but such an effect should be measurable in the visible.

Smithard[5] studied samples of Na in NaN_3 with the axis of symmetry perpendicular to the surface, since NaN_3 grows in thin plates and cleaves with the largest face in this orientation. The wavelength for maximum absorption depends on the annealing time, which is thought to be related to the mean particle size. The minimum measured wavelength for the peak was about 5200 Å. Smithard ignored the anisotropy of NaN_3 in his model. For Drude Na with the parameters given above and a relaxation time corrected for boundary scattering[14] by the conduction electrons $\tau = (\tau_B^{-1} + v_F/a)^{-1}$ with bulk relaxation $\tau_B = 3.36 \times 10^{-14}$ s, Fermi velocity $v_F = 1.03 \times 10^8$ cm/s, and particle radius $a = 15$ Å in an isotropic dielectric with constant $\epsilon_0 = 1.904$, Eq. (12) predicts a resonance at 5034 Å. Smithard's somewhat more complicated model yields 5020 Å for the peak. Taking the anisotropy of NaN_3 into account, the predicted resonance for Drude Na particles is at 5147 Å in substantially better agreement with experiment. The remaining red shift of the measured peak is about the same size as found by Smithard and Tran[12] for Na particles in isotropic NaCl. Several mechanisms[3,15–19] have been proposed to explain the increasing red shift with decreasing particle size for very small particles.

A disadvantage with the Na in NaN_3 system is that the particles have not yet been examined under an electron microscope to determine sizes and shapes. If the particles are oriented ellipsoids of revolution, rather than spheres, there are two resonance frequencies,

$$\omega_i = \omega_p / [\epsilon_\infty + (L_i^{-1} - 1)\epsilon_0]^{1/2} , \tag{17}$$

where the subscript $i = \parallel, \perp$ identifies the principal axes. The depolarization factors L_i are given by Eqs. (5) and (6) with $\epsilon_\parallel/\epsilon_\perp$ replaced by $(d_\perp/d_\parallel)^2$, where $d_\parallel$ and $d_\perp$ are the axes of the ellipsoid parallel and perpendicular to the direction of uniaxial symmetry. The absorption spectrum for oriented ellipsoidal particles with only a 1% difference between the lengths of the two axes would show a splitting comparable in magnitude to the prediction for Na in NaN_3, for which $\sqrt{\epsilon_\parallel/\epsilon_\perp} = 1.10$. The difference is due to the replacement of $\epsilon_\perp$ and $\epsilon_\parallel$ in Eqs. (13) and (16) by ϵ_0 in Eq. (17). Such a small ellipticity would be difficult to measure by electron microscopy.

In conclusion, this paper generalized the Maxwell-Garnett effective-medium theory to include the case of small spherical metal particles embedded in a uniaxial dielectric. Explicit expressions for the absorption coefficient obtained for low volume fractions of metal provide improved agreement with published experimental results on Na in NaN_3. This type of system could be used to study the effect of the dielectric constant of the host on the optical properties of the particles, but the samples must be well characterized and controlled with respect to morphology to avoid competing effects due to ellipticity of the particles.

ACKNOWLEDGMENTS

This work was supported by the National Science Foundation under Grant No. DMR-81-06097 and by the Air Force Research Office under Grant No. AFOSR-81-0121F (Materials Science Center Report No. 5385).

[1] G. Mie, Ann. Phys. (Leipzig) 25, 377 (1908).
[2] A. E. Hughes and S. C. Jain, Adv. Phys. 28, 717 (1979).
[3] R. P. Devaty and A. J. Sievers, Phys. Rev. B 24, 1079 (1981).
[4] J. C. Maxwell-Garnett, Philos. Trans. R. Soc. London 203, 385 (1904); 205, 237 (1905).
[5] M. A. Smithard, Solid State Commun. 14, 407 (1974).
[6] L. D. Landau and E. M. Lifshitz, *Electrodynamics of Continuous Media* (Pergamon, Oxford, 1960), pp. 315–324.
[7] M. Born and E. Wolf, *Principles of Optics*, Fifth ed. (Pergamon, Oxford, 1975), pp. 665–681.
[8] M. Born and E. Wolf, in *Principles of Optics*, Ref. 7, pp. 708–713.
[9] L. D. Landau and E. M. Lifshitz, in Ref. 6, problem 6, p. 62 and pp. 20–27.
[10] W. L. Bragg and A. B. Pippard, Acta. Crystallogr. 6, 865 (1953).
[11] R. W. Dreyfus and P. W. Long, Proc. R. Soc London Ser. A 246, 233 (1958).
[12] M. A. Smithard and M. Q. Tran, Helv. Phys. Acta 46, 869 (1974).
[13] N. V. Smith, Phys. Rev. Lett. 21, 96 (1968); Phys. Rev. 183, 634 (1969).
[14] U. Kreibig and C.v Fragstein, Z. Phys. 224, 307 (1969).
[15] G. Mukhopadhyay and S. Lundqvist, Solid State Commun. 44, 1379 (1982).
[16] P. Apell and A. Ljungbert, Solid State Commun. 44, 1367 (1982).
[17] R. Ruppin, J. Phys. Chem. Solids 39, 233 (1978); J. Opt. Soc. Am. 66, 449 (1976).
[18] A. D. Boardman and B. V. Paranjape, J. Phys. F 7, 1935 (1977).
[19] P. Ascarelli and M. Cini, Solid State Commun. 18, 385 (1976).

VOLUME 54, NUMBER 10 PHYSICAL REVIEW LETTERS 11 MARCH 1985

Effect of Melting of the Metallic Component on the Anomalous Far-Infrared Absorption of Superconducting Sn Particle Composites

W. A. Curtin, R. C. Spitzer, N. W. Ashcroft, and A. J. Sievers
Laboratory of Atomic and Solid State Physics and Materials Science Center, Cornell University, Ithaca, New York 14853
(Received 20 September 1984)

By means of a simple experimental heat-treatment procedure, the anomalous far-infrared absorption of superconducting Sn particle composites is shown to be associated with clustering. The structural insights thus obtained lead to a new theory in which the composite electric dipole absorption is dominated by poorly conducting clusters and is much larger than that of isolated metal particles. For superconducting particles, the theory predicts the absorption at frequencies above the gap frequency to be larger than in the normal state, in agreement with experiment.

PACS numbers: 74.30.Gn, 78.30.−j, 78.65.Ez

Recent experiments by Carr, Garland, and Tanner[1] on granular superconducting samples of small Sn particles embedded in an insulating alkali halide host have shown that not only is the absorption anomalously large in comparison to the predictions of classical theories,[2,3] but at frequencies higher than the superconducting gap frequency ω_g the composites are actually more absorbing in the superconducting state than in the normal state. Though carried out on a different class of system, the experimental work of Devaty and Sievers suggests that in the normal state this large absorption is a multiparticle effect.[4] The superconducting behavior is surprising since bulk Sn has smaller electromagnetic absorption in the superconducting state.

In this paper we (i) report far-infrared absorption measurements for composite samples comprised of either oxide-coated or oxide-free Sn particles in KBr at low temperatures, and (ii) present a new theory that accounts for the absorption in these systems. With respect to the measurements, we have found that both types of system show greater absorption in the superconducting state than in the normal state at frequencies higher than ω_{gap}. However, as we shall see below, after heat treatment, a process presumed to change the local particle topology, the absorption in the superconducting state is found *never* to exceed that of the normal state. The structural implications of these results suggest a new theoretical description of such systems. In particular, the unheated-sample results may now be understood by the assumption that the absorption is attributable to clusters of metal particles with effective dielectric properties which depend on the local particle topology. One particular cluster topology (the cluster percolation model) is most likely to be appropriate for the unheated composites. It is characterized by poorly conducting clusters (as compared to that of the metal particle constituents) and leads to large electric dipole (ED) absorption because of the dependence of the absorption on the inverse of the cluster conductivity in the ED mechanism. The superconducting anomaly then arises quite naturally for the ED absorption mechanism.

The Sn particles used in this study are produced by a method of inert-gas evaporation.[5] Sn metal is evaporated from a molybdenum boat in either a 20% oxygen: 80% argon or a 100% argon atmosphere at a pressure of 0.7 Torr. The particles prepared in the presence of the oxygen have a thin oxide coating which prevents them from cold welding together during the evaporation process. These samples are chosen to be similar to those studied by Carr, Garland, and Tanner. Particles made in a pure argon atmosphere are assumed to have no oxide coating. A scanning transmission electron microscope is used to measure the particle sizes: The oxide-coated and oxide-free particles discussed here have mean radii of 50 Å (including the oxide coating of[1] ≤ 20 Å) and 250 Å, respectively. Our samples are pressed pellets[1] of Sn particles embedded in a KBr host. The metal volume fill fraction is 0.02. Because of continuous radiation damage to the alkali halide as well as sample thinning problems, neither we nor others before us have been able to make direct TEM studies of the sample morphology.

Several of the composite samples were subjected to the heat treatment process mentioned above. This consists of heating the finished pellets for 15 min at a temperature of 250°C, which *exceeds* the bulk Sn melting point of 232 °C but is still well below the melting point of KBr. Either air or hydrogen atmosphere is used in heat treating of the oxide-free samples. Hydrogen is used to inhibit the formation of an oxide coating. Identical absorption coefficients are obtained for these different atmospheres. An air atmosphere is used exclusively in heat treating of the oxide samples. The Sn particles from the heat-treated samples were later examined with a TEM after removal of the alkali halide host with water. The micrographs show numerous large Sn single crystals with mean radii of 500 and 800 Å embedded in relatively large structureless 2000–3000 Å Sn clusters for the heated oxide and oxide-free samples, respectively.

Transmission spectra were measured from 4 to 30 cm^{-1} with a lamellar grating interferometer and a cry-

ostat with a ^{3}He-cooled germanium bolometer.[4] The infrared absorption coefficient is then calculated from the measured transmission coefficient $T(\omega)$ by

$$\alpha(\omega) = (1/t)\ln T(\omega) + \alpha_0,$$

where t is the thickness of the sample and α_0 is chosen so that the absorption coefficient extrapolates to 0 at zero frequency.

The normal-state absorption coefficient for representative unheated and heated oxide-coated and oxide-free samples is shown in Fig. 1. In complete agreement with previous studies of FIR absorption by small particles in alkali-halide hosts, the magnitude of α_n is orders of magnitude larger than predicted by simple theories. Here, both types of unheated samples show nearly quadratic frequency dependence at low frequencies but the oxide-coated sample data becomes nearly linear in frequency above 15 cm^{-1}. Upon heat treatment, the normal-state absorption of the oxide samples changes only slightly. However, the absorption of the oxide-free samples decreases by about a factor of 2 in magnitude and the frequency dependence is between linear and quadratic.

The superconducting-state results are also interesting: Distinct changes in the difference absorption $\Delta\alpha = \alpha_n - \alpha_s$ appear for both sample types upon heat treatment as shown in Fig. 2. Before heating, both sample types exhibit a superconducting absorption which is larger than the normal-state absorption above $\omega_g = 9.3$ cm^{-1}, as also reported by Carr, Garland, and Tanner. At frequencies below ω_g, $\Delta\alpha$ for the oxide-coated samples is small and its sign varies from sample to sample. But, for the oxide-free samples $\Delta\alpha$ is definitely positive. After heat treatment, the oxide-coated samples give $\Delta\alpha \approx 0$ over all of the frequency range studied. In contrast, $\Delta\alpha$ for the oxide-free samples becomes positive at all measured frequencies.

The changes in both α_n and $\Delta\alpha$ induced by the heat treatment are taken as strong evidence that clustering is indeed responsible for the anomalous FIR absorption in these systems. Our observations of large fused clusters present in the heat-treated samples suggest a general picture of the composite topology in which compact clusters of metal particles with effective local dielectric functions ϵ are distributed evenly throughout the host medium. We now describe the theory of one such cluster topology (the cluster percolation model), appropriate to the *unheated* samples, which predicts very large electric dipole absorption.

In the cluster percolation model, the composite is assumed to consist of dispersed clusters, on a size scale of a few thousand angstroms, embedded in the alkali halide host. Each cluster is itself a subcomposite consisting of metal particles of radius a, voids, and impurities and/or oxides. The latter serve to electrically isolate a fraction $1-p$ of the metal particles from their neighbors. The remaining metal particles in the cluster are taken to be electrically coupled

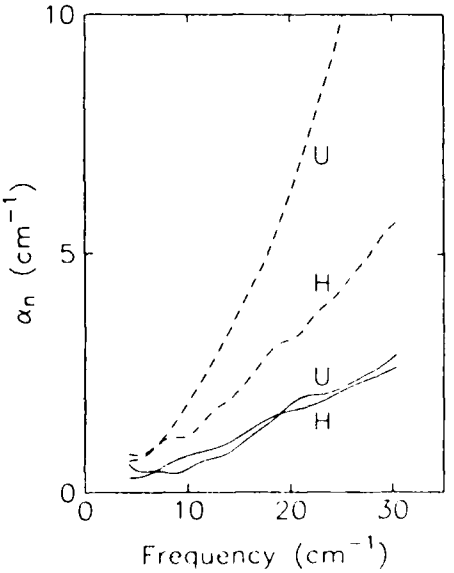

FIG. 1. Normal-state absorption coefficient α_n for oxide-coated (solid lines) and oxide-free (dashed lines) samples before (U) and after (H) the heat-treatment process. All the α_n are anomalously large with respect to previous theoretical predictions. The uncertainties in the measured α are $\pm 5\%$.

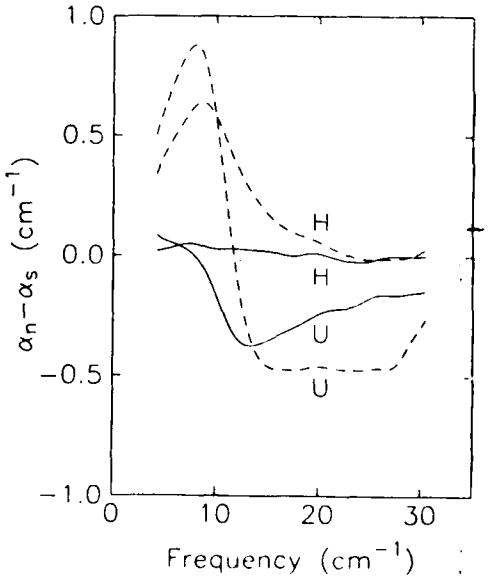

FIG. 2. Difference absorption $\Delta\alpha = \alpha_n - \alpha_s$ for oxide-coated (solid lines) and oxide-free (dashed lines) samples before (U) and after (H) heat-treatment process. Note the disappearance of the $\Delta\alpha(\omega > \omega_g) < 0$ anomaly seen by Carr, Garland, and Tanner upon heat treatment.

to an extent appropriate for a finite-sized system of metal particles of fill fraction p and complex dielectric $\epsilon_m(\omega)$ embedded in a nonconducting cluster host with dielectric ϵ_b. The cluster is characterized by an effective dielectric function $\epsilon(p,\omega)=\epsilon'(p,\omega)+i\epsilon''(p,\omega)$. The composite is an assembly of clusters with a range of p values. Clusters with p near 1 are very metallic and have small electric dipole absorption. Clusters with p near 0 consist of isolated metal particles and their absorption is again small, being similar to that of a system of small isolated particles. However, for clusters with p near the threshold for percolation, p_c, the electrically coupled metal particles will form tenuous chains and the absorption of such clusters is greatly enhanced relative to single particles.

The clusters with their associated $\epsilon(p,\omega)$ are assumed to be uniform in size and much smaller than the wavelength of the incident radiation. In addition, since the total metal fill fraction is $f \ll 1$, the fill fraction of each "bin" of clusters, $fN(p)dp$, where $N(p)$ is the fraction of clusters with conducting-element fill fraction between p and $p+dp$, is also necessarily small. Within these limits, the multicomponent Maxwell-Garnett[3,6] dielectric function for a dilute collection of spherical inclusions is then applicable, and leads to

$$\epsilon_{\text{comp}}(\omega)=\epsilon_h\left[1+3f\int dp\, N(p)\frac{\epsilon(p,\omega)-\epsilon_h}{\epsilon(p,\omega)+2\epsilon_h}\right], \quad (1)$$

where ϵ_h is the KBr host dielectric constant. The absorption coefficient arising from electric dipole absorption is $\alpha(\omega)=2(\omega/c)\text{Im}\epsilon_{\text{comp}}^{1/2}$ and is approximately given by

$$\alpha(\omega)\approx 9f\epsilon_h^{3/2}\frac{\omega}{c}\int dp N(p)\frac{\epsilon''(p,\omega)}{\epsilon'(p,\omega)^2+\epsilon''(p,\omega)^2}. \quad (2)$$

Large absorption results if there exist clusters with $\epsilon'\approx\epsilon''\ll\epsilon_m''$, a condition we will show to be generally satisfied. The distribution function $N(p)$ is not in general explicitly known. However, we expect $N(p)$ to be relatively featureless over the scale of the substantial variations in the dielectric function anticipated at $p\approx p_c$. By way of example, we have chosen $N(p)$ to be a constant over $0<p<0.30$ and zero elsewhere, a choice which provides merely an overall scale factor for the absorption.

To calculate the effective dielectric function $\epsilon(p,\omega)$ of a single cluster characterized by a chosen p, the structure is geometrically modeled as a simple cubic lattice spacing $2a$ and edge length L. Between the sites of the lattice are placed dielectric bonds assigned a dielectric constant of either $\epsilon_m(\omega)$ or ϵ_b with the fraction of p of $\epsilon_m(\omega)$ bonds corresponding to the volume fraction of unisolated metal particles. The metal dielectric function is assumed describable by a Drude model with an electron relaxation time $\tau=a/v_f$. The cluster host dielectric constant ϵ_b has contributions from the coated metal particles and is taken to be a real constant. An effective $\epsilon(p,\omega)$ may then be calculated in principle for the model cluster by averaging over the many possible configurations of conducting and nonconducting bonds at fixed p. This lengthy procedure can, however, be avoided by employing a real-space renormalization-group (RSRG) technique[7] to calculate $\epsilon(p,\omega)$. For a finite system, the RSRG transformation, which reduces the number of bonds along a cube edge by a factor of 2 after each transformation, is truncated after $\ln(L/2a)/\ln(2)$ iterations so that an $L\times L\times L$ cluster with fraction p of $\epsilon_m(\omega)$ bonds is reduced to a single effective cluster of dielectric $\epsilon(p,\omega)$.

Utilizing this approach, we find that the real part of $\epsilon(p,\omega)$ increases slowly with increasing p; in contrast, the imaginary part increases very rapidly from values much less than the real part to values much greater than the real part, over a fairly narrow $(0.1<p<0.25)$ range of p. This transition constitutes the remnant of the insulator-metal transition of infinite clusters and guarantees that the absorption coefficient [see Eq. (2)] will have contributions from clusters with $\epsilon'(p,\omega)=\epsilon''(p,\omega)\ll\epsilon_m''(\omega)$, as is necessary for large absorption. The frequency dependence of $\alpha(\omega)$ is sensitive to the details of the calculation of $\epsilon(p,\omega)$ but our model results should be a reasonable representation of the actual $\epsilon(p,\omega)$ and the resultant absorption coefficient. We emphasize that the general behavior of $\epsilon(p,\omega)$ and hence α is expected for any type of calculation incorporating the essential physics. The RSRG technique merely puts the transition of $\epsilon(p,\omega)$ from insulating to metallic behavior in a particular range of p with a (size-dependent) width and frequency dependence.

The absorption coefficient versus frequency as calculated by Eq. (1) [with $\epsilon(p,\omega)$ as appropriate for $a=50$ Å Sn particles in clusters of sizes $L=64a=3200$ Å] is presented in Fig. 3. The parameters have been chosen to correspond to the unheated oxide-coated samples studied here with $\epsilon_b=10$. The magnitude of the absorption at low frequencies is fairly large: $\alpha(8\text{ cm}^{-1})\approx 0.075\text{ cm}^{-1}$, which is within a factor of 4 of the measured value and exceeds the Maxwell-Garnett single-particle estimates by about 3 orders of magnitude. The frequency depedence is also in good agreement with the data.[8] The magnitude of α is fairly insensitive to the magnitude of $\epsilon_m''(\omega)$ and nearly proportional to $\epsilon_b^{-1/2}$.

For the superconducting state, the composite absorption coefficient may be calculated with the same procedure but with the use of the Mattis-Bardeen[9] dielectric function for the superconducting metallic

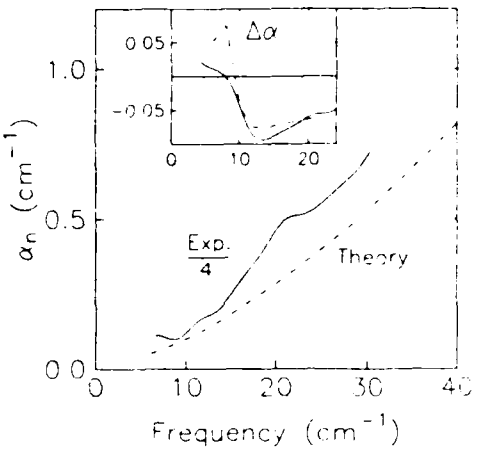

FIG. 3. Normal-state absorption coefficient in cluster percolation model (dot-dashed lines), for clusters of size $L = 3200$ Å, particle diameter $2a = 100$ Å, corresponding to the non-heat-treated oxide-coated samples studied here. Inset: $\Delta\alpha(\text{cm}^{-1}) = \alpha_n - \alpha_s$ vs $\omega(\text{cm}^{-1})$ calculated with the same model with $\omega_g = 8$ cm^{-1}. The measured α_n and $\Delta\alpha$ for unheated oxide samples of Figs. 1 and 2 scaled down by an arbitrary factor of 4 are also shown (solid lines).

component. The difference absorption $\Delta\alpha$, shown in the inset of Fig. 3, exhibits a positive peak near ω_g (taken to be at 8 cm^{-1}) and a negative peak at a higher frequency followed by a decrease in $\Delta\alpha$ to zero at $\omega >> \omega_g$. The calculated $\Delta\alpha$ is quite consistent with experimental observations. The "anomalous" (i.e., $\Delta\alpha < 0$) absorption results directly from the form of Eq. (2). In the superconducting state, ϵ'' is reduced from its normal-state value and ϵ' increased such that the absorption is actually increased relative to that of the normal state for $\omega > \omega_g$.

Upon heat treatment, we expect the metal particles in each cluster to fuse together despite the presence of the coating on some preheated particles. Fusion represents a drastic change in the cluster topology and should consideralby alter the character of the absorption coefficient. In particular, we expect the oxide-free sample clusters to become quite metallic and exhibit large magnetic dipolelike absorption upon heat treatment, yielding $\Delta\alpha > 0$ above ω_g.[10] However, for the oxide-coated samples, the presence of the oxide must prevent a complete transition from the cluster percolation topology to a fused metallic cluster topology and $\alpha(\omega)$ should then result from a combination of the mechanisms just described.

In summary, heat treatment of metal–alkali-halide composites greatly affects their absorption coefficients and eliminates the $\Delta\alpha < 0$ superconducting "anomaly." A cluster percolation model, in which the connectivity within a cluster is sensitive to the melting of the metal component, leads to clusters some of which satisfy a resonance condition $\epsilon' \approx \epsilon''$ in the absorption with ϵ' and ϵ'' much smaller than ϵ_m''. The resulting absorption coefficients are in good agreement with experiment, resolving not only the $\Delta\alpha < 0$ anomaly of Carr, Garland, and Tanner but also the long-standing discrepancy of orders of magnitude difference between theory and experiment in such systems.

We wish to thank Dr. S. Solla for many helpful discussions. This work was supported by the National Science Foundation under Grant No. DMR-81-06097 and under Grant No. DMR-81-06097 through the Materials Science Center at Cornell University (MSC Report No. 5406), and by the Air Force Office of Scientific Research under Grant No. AFOSR-81-0121F.

[1]G. L. Carr, J. C. Garland, and D. B. Tanner, Phys. Rev. Lett. **50**, 1607 (1983).

[2]G. Mie, Ann. Phys. **25**, 377 (1908).

[3]J. C. Maxwell-Garnett, Philos. Trans. Roy. Soc. London **203**, 385 (1904).

[4]R. P. Devaty and A. J. Sievers, Phys. Rev. Lett. **54**, 1 (1984).

[5]C. G. Granqvist and R. A. Buhrman, J. Appl. Phys. **47**, 2200 (1976).

[6]J. Bernasconi, Phys. Rev. B **18**, 2185 (1978); S. Solla, to be published.

[7]D. M. Wood and N. W. Ashcroft, Philos. Mag. **35**, 269 (1976).

[8]Calculations for clusters with $L/2a = 16$ yield an absorption coefficient larger in magnitude but weaker in ω dependence than that for $L/2a = 32$.

[9]D. C. Mattis and J. Bardeen, Phys. Rev. **111**, 412 (1958).

[10]W. A. Curtin and N. W. Ashcroft, Phys. Rev. B **31**, 3287 (1985). Calculations of α for the oxide-free samples in the unheated (cluster percolation model) and heat-treated (magnetic dipole fused cluster model) states are in good agreement with results presented here.

Absorptivity of $CePd_3$ from 5 to 400 meV

B. C. Webb and A. J. Sievers
Laboratory of Atomic and Solid State Physics and Materials Science Center, Cornell University, Ithaca, New York 14853

T. Mihalisin
Department of Physics, Temple University, Philadelphia, Pennsylvania 19122

The far infrared absorptivity of $CePd_3$ has been measured between 4.2 and 300 K over a photon energy range which is an order of magnitude larger than previously reported. These measurements together with previous results map out the entire region of the low-temperature $CePd_3$ absorptivity anomaly, which is larger and extends to larger energies than extrapolation from earlier cavity measurements would suggest. The anomaly is too large to be compatible with simple conduction electron scattering off a resonant level near the Fermi energy. Above 200 meV only a weak temperature dependence is observed although a minimum in the absorptivity at 270 meV, attributed to an *f* multiplet transition, appears to sharpen at the lowest temperatures.

Nonresonant far infrared cavity techniques[1,2] previously have been used to identify an unusual temperature dependent absorption feature centered at about 20 meV in the mixed valence compound $CePd_3$. This low-temperature anomaly appeared to be consistent with a model[1,3,4] which includes energy-dependent electron scattering off a resonant level near the Fermi energy.

We have made direct measurements of the reflectivity of $CePd_3$ between 4 and 300 K over the photon range 10–400 meV, thereby extending the range of the earlier measurements by an order of magnitude in energy. Our results indicate that at higher energies the cavity measurements lead one to underestimate both the width and strength of the low-temperature absorption feature. These new data are not compatible with a simple resonant level model.

At energies greater than about 12 meV the absorptivity of $CePd_3$ at 4.2 K is large enough so that it can be obtained from a straightforward reflectivity measurement while for smaller energies nonresonant cavities have been used. In the energy region from 12 to 40 meV the two measurement techniques can be compared. Our measurements were made as follows.

5–40 meV: Nonresonant cavity techniques have been used which are similar to those described earlier.[2] Radiation from a Michelson interferometer propagates down a light pipe into a cryostat through a nonresonant cavity and to the detector. Different samples are sequentially attached to the cavity wall and the far infrared transmission compared.

12–125 meV: The cavity is now replaced by a section of light pipe which contains two right-angle bends at which samples are introduced. The sample assembly can be rotated to substitute in place an identical arrangement with Au-coated reference samples. The interferometer resolution is 2 meV for energies below 50 and 6 meV at larger energies. The absorptivities are reproducible to ± 0.02.

125–400 meV: Two samples are mounted in an immersion optical access cryostat which contains ZnSe windows. The entire assembly is inserted in the beam of a commercial Michelson interferometer which is scanned at a resolution of 0.4 meV. The beam is reflected off each sample at 45° and returned to its original path by another pair of mirrors. This allows the sample to be introduced into the optical path without deviating the beam. The relative error in the measured absorptivities is estimated to be ± 0.03. To fix the absolute magnitude of the absorptivity the P34 line of the 10-μm branch of a CO_2 laser (115 meV) is used for a single-frequency measurement of the temperature and polarization dependence.

The cavity data and the specular reflectivity data are compared at two temperatures in Fig. 1. The measurements agree at the lower end of the frequency range but disagree at the higher frequency end. Both measurements are seen to be well above the Drude theory value. In the Drude model for a

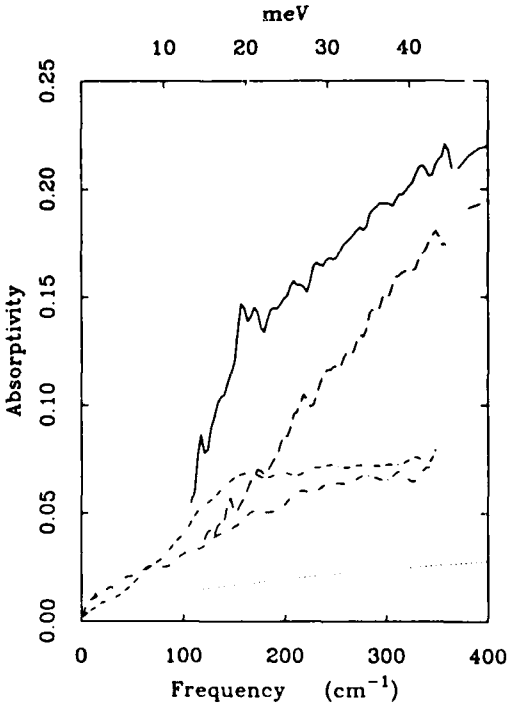

FIG. 1. Absorptivity of $CePd_3$ as a function of frequency for two temperatures. The absorptivity has been measured using two different experimental methods: reflectivity (solid curve 4 K, dashed curve 75 K), cavity (dash-dash-dot 4 K, dash-dot 75 K). The dotted curve is from the Drude model for $CePd_3$ at 4 K with $\omega\tau \gg 1$ and $\rho = 12\ \mu\Omega$ cm.

 0021-8979/85/013134-03$02.40

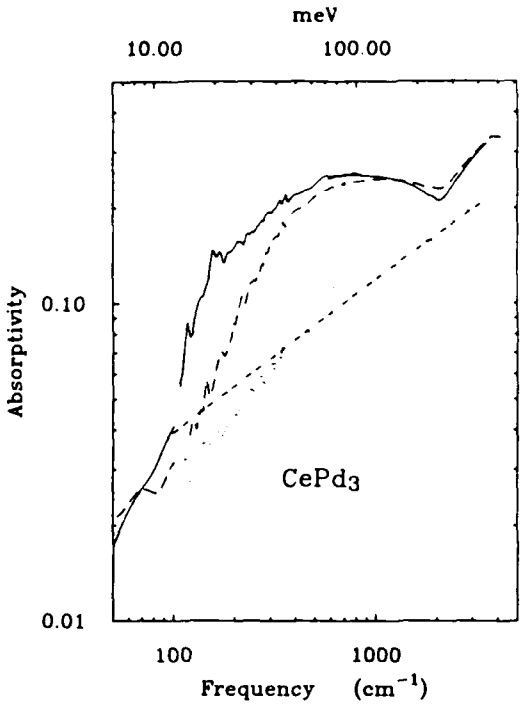

FIG. 2. Absorptivity of $CePd_3$ as a function of temperature over an extended frequency interval. The solid curve is for 4 K; the dashed curve, 75 K; and the dotted curve, 300 K. The dash-dot curve is the Drude theory curve for $CePd_3$ at 300 K with $\rho = 120\,\mu\Omega$ cm and $\omega\tau \ll 1$.

free electron metal the dielectric function is

$$\epsilon(\omega) = 1 + \frac{i4\pi\sigma_0/\omega}{1 - i\omega\tau_0}. \tag{1}$$

For a high-resistivity metal $\omega\tau_0 \ll 1$ in this region and the dielectric function and absorptivity are dependent only on the conductivity σ_0. The Drude curve shown is for a sample at 4 K measured to have a resistivity of $12\,\mu\Omega$ cm. The differences between the observed absorption and the Drude model diminish for both types of measurements as the temperature increases.

Figure 2 shows the frequency dependent absorptivity of $CePd_3$ at three different temperatures. Our room temperature measurement is in agreement with the earlier work of Allen.[5] The absorptivity is roughly fit by the Drude model up to 100 meV with an amplitude consistent with the resistivity of $CePd_3$ at 300 K, $120\,\mu\Omega$ cm. As the temperature is lowered the absorptivity increases, gradually developing the sharp absorption edge at about 12 meV. At 4 K the absorption is fairly constant between 75 and 200 meV but a sharp notch is observed at 260 meV. Hillebrands[6] has attributed a feature in this energy region at 300 K to the spin-orbit split multiplet transition $^2F_{5/2} \rightarrow {}^2F_{7/2}$ at 270 meV.

A phenomenological model which includes resonant scattering of conduction electrons from a level near the Fermi energy has been proposed to account for the anomolous absorption at low temperatures. The resonance effect can be modeled by replacing the electron scattering rate $1/\tau_0$ in the Drude model with an energy-dependent rate

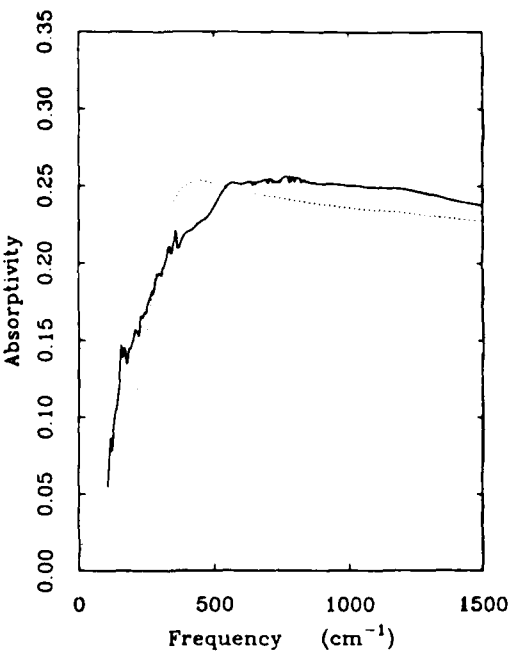

FIG. 3. Fit of the resonant scattering model to the absorptivity of $CePd_3$ at 4 K. Data: solid curve; fit: dotted curve. The fitting parameters are listed in Table I.

$$\frac{1}{\tau(\omega)} = \frac{1}{\tau_0} + \frac{S\Gamma}{\hbar\omega - E_0 + i\Gamma}. \tag{2}$$

This functional form produces a peak in the absorptivity near $\hbar\omega = E_0$. This model is described in more detail in Ref. 4.

Figure 3 shows our best fit with the fitting parameters listed in Table I. The model fails in two ways. It is not possible to fit both the sharp onset at 12 meV and also the more rounded maximum in the absorptivity. Also, and more importantly, inspection of Table I shows that the contribution of the resonance to the dc resistivity (ρ_{dc}) increases the resistivity to $150\,\mu\Omega$ cm, far above the observed value at 4 K (12 $\mu\Omega$ cm) and near the maximum resistivity for $CePd_3$ of 170 $\mu\Omega$ cm at 130 K. Also shown in this table are the parameters obtained from the earlier cavity measurements over a restricted frequency interval. The fortuitous agreement for ρ_{dc} has lent support to the resonant scattering model.

In conclusion, at the lowest frequencies measured, the absorptivity agrees with Drude model predictions but at the larger far infrared frequencies the temperature-dependent anomaly, which is characterized by excess absorption at 4.2

TABLE I. Parameters of the resonant scattering model fits.

Data	E_0	Γ (meV)	S/ω_p^2 (eV^{-1})	$\omega_p^2\tau_0$ (eV)	ρ_{dc} ($\mu\Omega$ cm)
Cavity*	6.32	1.61	0.0785	890	12
This work	14.88	5.0	0.20	890	150

*Ref. 4.

K, is stronger and extends to larger energies (~ 200 meV) than extrapolation from earlier cavity measurements would suggest. Theoretical mixed valence models must now account for an excess absorptivity with a sharp onset at 12 meV that continues up to 200 meV.

The work of B. C. Webb and A. J. Sievers has been supported by NSF Grant No. DMR-81-06097 and AFOSR under Grant No. AFOSR-81-0121F. The work of T. M. Mihalisin has been supported by NSF Grant No. DMR-82-19782. This is Cornell Materials Science Center Report No. 5418.

[1] F. E. Pinkerton, A. J. Sievers, J. W. Wilkins, M. B. Maple, and B. C. Sales, Phys. Rev. Lett. **47**, 1018 (1981).
[2] F. E. Pinkerton, A. J. Sievers, M. B. Maple, and B. C. Sales, Phys. Rev. B **29**, 609 (1984).
[3] F. E. Pinkerton, A. J. Sievers, J. W. Wilkins, M. B. Maple, and B. C. Sales, in *Valence Fluctuations in Solids*, edited by L. M. Falicov, W. Hanke, and M. B. Maple (North-Holland, Amsterdam, 1981).
[4] F. E. Pinkerton, B. C. Webb, A. J. Sievers, J. W. Wilkins, and L. J. Sham, Phys. Rev. B **30**, 3068 (1984).
[5] J. W. Allen, R. J. Nemanich, and S.-J. Oh, J. Appl. Phys. **53**, 2145 (1982).
[6] B. Hillebrands, G. Guntherodt, R. Pott, W. Konig, and A. Breitschwerdt, Solid State Commun. **43**, 891 (1982).

Bulletin of the American Physical Society

Program of the 1985 March Meeting in Baltimore, Maryland; 25–29 March 1985

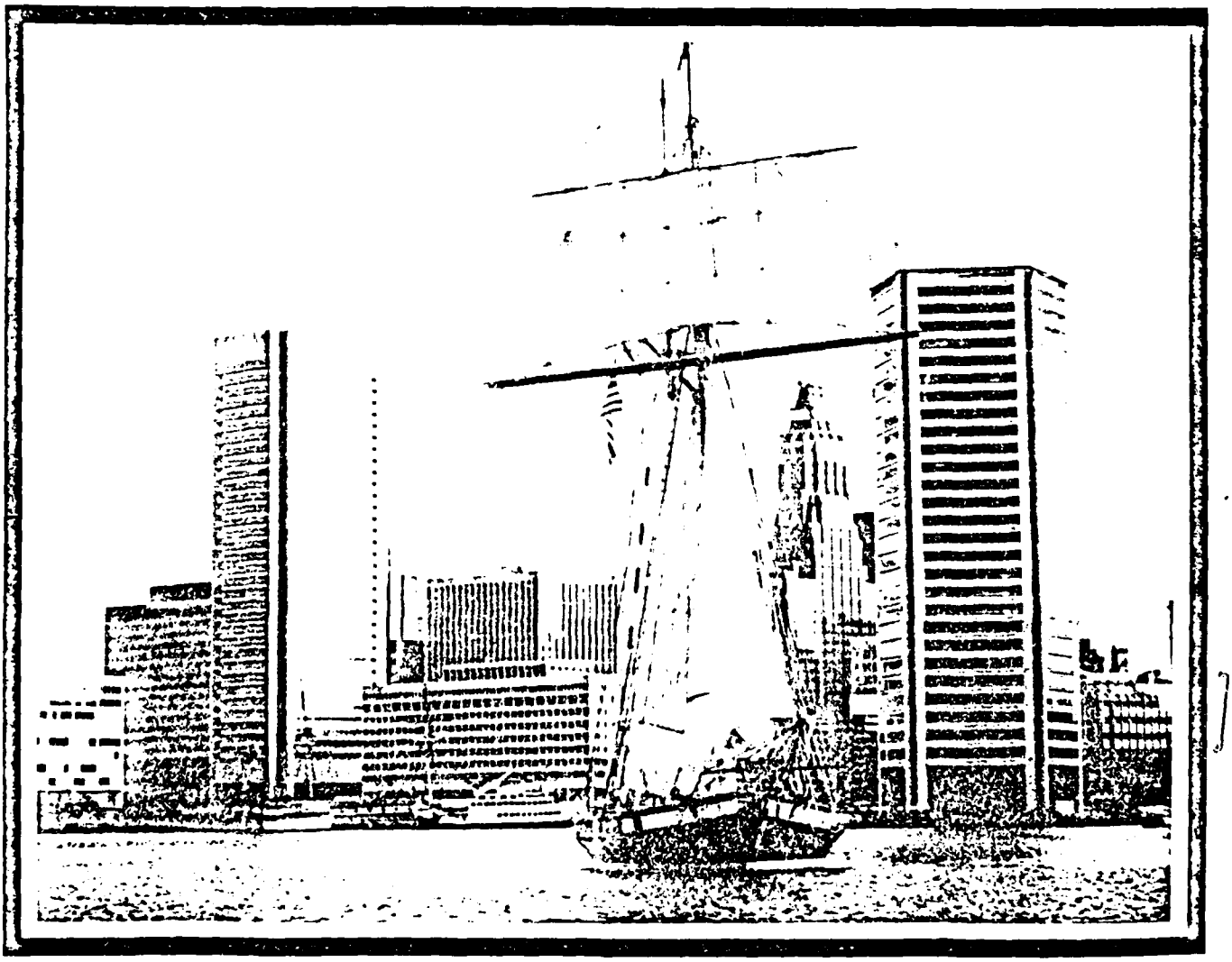

Volume 30, Number 3 **March 1985**

7.0-8.0x10^{4}cm^2/V•sec at 77K with carrier densities of 0.8-1.0x10^{12}cm^{-2}. The temperature dependence of the mobility below 77K is sensitive to growth conditions such as transient time from GaSb growth to InAs growth (or reverse) or growth temperature. This suggests that the electron scattering is due not only to residual impurities but also to roughness and/or alloying at the InAs/GaSb interface. The difference with respect to the GaAs/AlAs system may arise from the relatively large lattice mismatch between GaSb and InAs as well as between GaSb and the GaAs substrate.

*Sponsored in part by ARO Contract.

11:36

AE 14 2DEG in $In_{0.53}Ga_{0.47}As$/InP Heterostructures Grown by Atmospheric MOCVD, L. D. ZHU, P. SULEWSKI, K. T. CHAN, J. M. BALLANTYNE and A. J. SIEVERS, Cornell U.*--We have fabricated $In_{0.53}Ga_{0.47}As$/InP heterostructures by the method of metal organic chemical vapor deposition (MOCVD) at atmospheric pressure. These structures consist of a 0.7 μm thick n-type InP layer, a 3.5 μm undoped $In_{0.53}Ga_{0.47}As$ layer and a 0.3 μm n-type InP cap layer sequentially grown on a semi-insulating InP substrate using $(CH_3)_3In$ and $(CH_3)_3Ga$ as In and Ga sources. The electron mobility (cm^2/Vs) at 300 K and 3 K is 11,600 and 82,000 respectively, with a maximum value of 90,000 at 50 K. The temperature dependence confirms the two dimensional electron gas (2DEG) character and the low temperature values are about 2.9 times larger than those previously reported.[1] The combined sheet density for the two interfaces is 2.7x10^{11}/cm^2 at 4 K. Far infrared cyclotron resonance measurements indicate that m*/m=0.044 for this 2DEG. The measured linewidth of 1 meV is in reasonable agreement with the relaxation time determined from the mobility.

*Supported by AFOSR, NRRFSS and MSC at Cornell U.

[1]H. P. Wei et al., Appl. Phys. Lett. 45, 666 (1984).

11:48

AE 15 Electronic Specific Heat in GaAs/GaAlAs Multilayers. E. GORNIK, R. LASSNIG, G. STRASSER, Inst. of Exp. Physics, Univ. of Innsbruck, Austria. —We report the observation of the magnetic field dependent electronic specific heat in GaAs/GaAlAs multilayers. Samples with 172 and 94 double layers of 200 Å GaAs and 200 Å GaAlAs with mobilities of 40 000 cm^2/Vs and 80 000 cm^2/Vs respectively were investigated.
The temperature change of the 10 - 20 μm thick samples was measured with a evaporated Au-Ge film. The thermal isolation was achieved by 5 μm thick superconducting wires. A Ni-Cr film of 100 Å thickness was used as a heater.
Oscillations of the sample temperature in the order of nK were observed as a function of the magnetic field. Both, intra level and inter Landau level contributions are observed. Theoretical fits[1] to the data reveal evidence for a Gaussian density of states with a constant background density. For both samples a background density of 25 % was found. For the higher mobility sample a Gaussian width of 2.0 meV, for the lower mobility sample a width of 3.0 meV was determined.
[1]W. Zawadzki, R. Lassnig, Solid State Commun. 50, 537 (1984).

12:00

AE 16 Interfacial Disorder and Electron Transport in a Superlattice, N. TRIVEDI and N. W. ASHCROFT, Cornell U.*--We study the effects of interfacial disorder on electron transport in a superlattice. The interfaces between superlattice constituents are modeled as a periodic array of sheets in which the scattering centers are disordered with no correlation between sheets. By choice of field direction, the scattering effects can be separated into boundary scattering and junction transport components. A combination of standard linear response and diagrammatic methods have been used to derive the corresponding conductivity tensor for the weak scattering case. The results are investigated in detail for their sensitivity to the degree of correlation between the scatterers in a single sheet.

*Supported by the Semiconductor Research Corporation under contract #82-11-001.

SESSION AF: EPITAXY

Monday morning, 25 March 1985
Room 301 at 9:00
R. Tromp, presiding

9:00

AF 1 **Growth of HgCdTe and Other Hg-Based Films and Multilayers by Molecular Beam Epitaxy***, J.W. COOK, JR., K.A. HARRIS, AND J.F. SCHETZINA, N.C. State University--Growth of HgCdTe and other Hg-based films and multilayers by MBE presents special problems because of the high vapor pressure and small sticking coefficient of Hg. At NCSU, we have designed and constructed an MBE system specifically for growing Hg-based materials. The system consists of a main UHV chamber with provisions for seven MBE effusion sources with computer-controlled shutters, a UHV load-lock for introducing and retrieving samples from the main chamber, and a preparation and analysis chamber featuring a substrate preheat station (up to 1200 C), a sputtering station, an in situ metallization station, and a back reflection LEED facility. The Hg MBE source is designed for high temperature stability (+0.1 C at 200 C) and may be refilled without disturbing the UHV ambient. The system has been successfully employed to grow state-of-the-art CdTe epilayers on GaAs substrates. Results of initial HgCdTe film growth experiments will also be presented and discussed.

*Work supported by DARPA/ARO contract DAAG29-83-K-0102.

9:12

AF 2 High Resolution Electron Microscope Study of Epitaxial CdTe-GaAs Interfaces* N. OTSUKA, L. A. KOLODZIEJSKI, R. L. GUNSHOR, and S. DATTA, Purdue U.** and R. N. BICKNELL, and J. F. SCHETZINA, North Carolina State U.***--CdTe films have been grown on (100) GaAs substrates with two different epitaxial interfaces: (111)CdTe||(100)GaAs and (100) CdTe||(100)GaAs. High resolution electron microscope observation of these two types of interfaces was carried out in order to investigate the role of the substrate surface microstructure in determining which type of epitaxy occurs. The interface of the former type shows a direct contact between the CdTe and GaAs crystals, while the interface of the latter type has a very thin oxide layer (~10A in thickness) between the two crystals.
*Submitted by R. L. Gunshor
**Supported by Office of Naval Research Contract 014-82-K-0563 and the NSF-MRL Program under Grant DMR-83-16999.
***Supported by NSF Grant DMR-83-13036 and DARPA/ARO Contract DAAG 29-83-K-0102.

9:24

AF 3 Molecular Beam Epitaxy of $Zn_{1-x}Mn_xSe$. L. A. KOLODZIEJSKI, M. K. UDO, T. C. BONSETT, R. L. GUNSHOR, S. DATTA, R. B. BYLSMA, W. M. BECKER AND N. OTSUKA, Purdue U.*--Epitaxial single crystal thin films of the dilated magnetic semiconductor $Zn_{1-x}Mn_xSe$ have been grown by molecular beam epitaxy on GaAs substrates. Various Mn compositions have been grown with varying growth rates and substrate temperatures. Photoluminescence (PL) spectra of MBE films show fewer impurity-

SESSION DH: COMPOSITES I

Tuesday morning, 26 March 1985
Room 305 at 9:00
D. Tanner, presiding

9:00

DH 1 Effective Medium Model of Cermet Films with Large Metal Packing Fractions. D. E. ASPNES, Bell Communications Research, Inc., Murray Hill.--Recently reported optical properties of thermally evaporated Rh films cannot be understood by standard effective medium approaches, but can be described by the approximate analytic solution of a metal-rich cermet microstructure consisting of rectangular metal blocks coated with insulating films. The solution becomes exact in the limit of vanishing insulator packing fraction and can be used to derive an effective medium expression. This expression is shown to be equivalent to the Maxwell Garnett model with the insulator acting as the host phase. Since this result is valid even in the limit of zero insulator packing fraction, the model establishes that connectivity, not relative volume fraction, is the physical property determining the identity of the host phase. The model also establishes that the host dielectric function, the generalized coordinate representing connectivity, is equivalent in importance to the screening and relative volume fraction parameters in determining the dielectric properties of heterogeneous media.

[1] D. P. Arndt et. al., Appl. Opt. 23, 3571 (1984).

9:12

DH 2 Complex Dielectric Response of Metal Particle Clusters. P. M. Hui and D. Stroud, The Ohio State University. -- We introduce a self-consistent theory for the complex dielectric response of clusters of small metal particles. The theory is based on the assumption that the clusters have fractal dimensionalities, and leads to a cubic equation for the effective complex dielectric function. When applied to clusters of small metal particles in an insulating host, with reasonable assumptions about cluster size and fractal dimension, the theory predicts a far infrared absorption per unit volume of metal vastly in excess of the corresponding prediction of the Maxwell-Garnett approximation. An enhanced absorption due to eddy currents is also predicted. The possibility that the theory explains the anomalous far infrared absorption observed in composite materials is briefly discussed.

*Work supported by NSF through grant DMR 81-14842

9:24

DH 3 Theory of Far-Infrared Absorption in Metal Particle Composites.* W. A. CURTIN and N. W. ASHCROFT, Cornell U. -- Our theory for the anomalous far-infrared absorption in normal and superconducting metal particle composites agrees with the data on Sn. The theory assumes the composites to consist of metal particle clusters. The effective dielectric constant $\epsilon(p,\omega)=\epsilon'(p,\omega)+i\epsilon''(p,\omega)$ of a cluster is calculated for a model cluster with fractions p of metal particles and (1-p) of electrically isolated (coated metal) particles. The electric dipole absorption of a cluster depends on $\approx\epsilon''(\epsilon'^2+\epsilon''^2)$ and so the composite absorption is dominated by clusters with $\epsilon'\approx\epsilon''$, a condition satisfied at p for which $\epsilon''(p,\omega)\cdots\epsilon''_{metal}(\omega)$. The model composite absorption is thus much larger than that predicted by isolated particle theories. The large absorption is a general result of the cluster assumption, independent of the model employed to calculate $\epsilon(p,\omega)$. The anomalous superconducting absorption results from $\epsilon''(\epsilon'^2+\epsilon''^2)$ being larger in the superconducting state than in the normal state at frequencies above the gap frequency.

*Supported by the Materials Science Center at Cornell University.

9:36

DH 4 Infrared and Optical Studies of Small Metal Particles, Y.H. KIM and D.B. TANNER, University of Florida.--Measurements of the absorption in gas-evaporated Al and Ag particles have been made over frequencies between the far infrared (8 cm^{-1} or 1 meV) and the visible (35000 cm^{-1} or 4.3 eV). The particles had radii of order 100 Å and were supported in KCl or parrafin host. In accord with previous studies, the far-infrared absorption was larger than theoretical estimates. The Al particles had a broad absorption maximum at 900 cm^{-1} which could be modeled as due to a 10 Å thick Al_2O_3 surface layer. Above this frequency the absorption was substantially smaller; at higher frequencies there was structure due to an interband transition in Al metal. The Maxwell-Garnett resonance was observed in very dilute Ag composites at 24000 cm^{-1} (3 eV).

9:48

DH 5 **Optical Properties of Metal-Insulator Suspensions, V. A. DAVIS, *Brandeis U.* and L. SCHWARTZ, *Schlumberger-Doll Research*. -- Roth's effective medium approximation (EMA)[1], a self consistent multiple scattering method, is used to calculate the dielectric response of a system comprised of independent metallic grains embedded in an insulating host material. In particular, we consider Ag spheres, described by a Drude model, and a geletin host with $\epsilon_0 = 2.37$. Our aim is to show that, as the packing fraction of the grains is varied, a reasonable picture of the resonance structure in $\epsilon_{eff}(\omega)$ emerges naturally from a theory of *structurally* disordered composites. In this regard our calculations will be compared with the results of the quasicrystalline approximation (QCA)[2] and a recently proposed lattice-gas model.[3]**

[1] L. Roth, Phys. Rev. B9, 2476 (1974); V. A. Davis and L. Schwartz, Phys. Rev. (submitted).
[2] L. Tsang and J. A. Kong, J. Appl. Phys. 53, 7162 (1982).
[3] A. Liebsch and P. V. Gonzalez, Phys. Rev. B29, 6907 (1984).

10:00

DH 6 Observability of Quantum Size Effects in Small Metal Particles by Absorption Spectroscopy. R.P.DEVATY, U. of Pittsburgh, and A.J. SIEVERS, Cornell U.* -- The Gor'kov-Eliashberg model for far infrared absorption by small metal particles is reexamined. Although the oscillations in the absorption coefficient signifying discrete levels are washed out by the size distribution for presently available samples[1], nonquadratic frequency dependence persists below the mean Kubo gap. For a log normal distribution of 20Å diameter Au particles with σ=1.2, the crossover to a nonquadratic asymptote should be observable in the far infrared (2-100 cm^{-1}). The crossover is broadened by the size distribution, but the low frequency asymptote is obtained in the very far infrared or microwaves even if σ=1.6. The prediction of greater than quadratic low frequency asymptotes provides the possibility of an experimental test for quantum size effects.
[1]R.P. Devaty and A.J. Sievers, Phys Rev. B22, 2123(1980).
*Supported by the NSF under Grant #DMR-81-06097 and the Air Force under Grant #AFOSR-81-0121B.

10:12

DH 7 The Far-infrared Absorption of Small Silver Particles I.* Sung-ik Lee, Tae Won Noh, Kevin Cummings, J. R. Gaines, The Ohio State University. A new insulating host, teflon, was used to measure the far-infrared absorption of small silver particles. The silver particle

17:30
EJ 14 Static Phonon Dressing of Sine-Gordon Solitons on a Discrete Lattice. P. STANCIOFF, S. BURDICK, C. WILLIS, and M. EL-BATANOUNY, Boston U.*--The modifications incurred upon a continuum stationary Sine-Gordon soliton due to the discreteness of the underlying lattice are treated in terms of a static phonon dressing on the continuum solution. The results are compared with those obtained from molecular dynamics computations performed by us and similar calculations for ϕ^4 solitons published recently.[1] Our method of computation has been outlined previously.[2] On the basis of the phonon dressing picture we identify and discuss the sources of these modifications. Dynamics related quantities such as the Peierls-Nabarro barrier and the soliton pinning frequency are calculated and their correlation with the phonon dressing established. Finally, the importance of the present study for future treatment of discreteness related dynamical effects is pointed out.

*Supported by DOE Contract #DE-AC02-83ER45029.

[1] J. Andrew Combs and Sidney Yip, Phys. Rev. B28, 6823 (1983).
[2] R.M. Martini, S. Burdick, M. El-Batanouny and G. Kirczenow, Phys. Rev. B30, 492 (1984).

17:42
EJ 15 First SEW Observation of Surface Reconstruction on W(100). D.M. RIFFE, L. M. HANSSEN and A. J. SIEVERS, Cornell U.*--We have studied the effects of H_2 and D_2 adsorption on the transmission of Surface Electromagnetic Waves (SEW's) on W(100) in the 10μ region. LEED and thermal desorption have been used to characterize the surface. Large changes in transmission are observed for coverages smaller than saturated coverage (θ=1). As a function of θ the signature of this effect at all frequencies studied from 886 cm^{-1} to 1080 cm^{-1} is as follows: Initially, H_2 or D_2 adsorption increases the SEW transmission to a sharp maximum at θ=0.21±.02 (e.g. for H_2 at 997 cm^{-1}, a 16% increase from θ=0 level). But with further adsorption the transmission decreases, passing through its initial value at θ=0.33±0.03 and reaching a broad minimum at θ=0.62±0.05 (13% decrease from θ=0 level). The signal then rises until θ=1, but a net decrease remains (5.7%). Dramatic effects[1] have been observed with a variety of experimental probes at θ=0.2 where LEED studies show a transition from a split c(2x2) pattern to a streaked c(2x2) pattern. Our measurements demonstrate that this is also the case with SEW's.

*Supported by AFOSR and NSF.

[1] D.A. King and G. Thomas, Surf. Sci. 92 (1980) 201.

SESSION EJ: SEMICONDUCTOR SURFACES II

Tuesday afternoon, 26 March 1985
Room 321 at 14:30
D. J. Chadi, presiding

14:30
EJ 1 First Principles Investigation of Location and Electronic Structures of Bromine Atoms Chemisorbed on Si(111) Surface. S.M. MOHAPATRA, N. SAHOO, K.C. MISHRA, B.N. DEV, W.M. GIBSON and T.P.DAS, SUNY/Albany.--Self-consistent Field Hartree-Fock Cluster investigations have been carried out for bromine atoms chemisorbed on Si(111) surface using 5, 14 and 27 atom clusters. The Si-Br bond lengths were determined through minimization of the total energy of the clusters. Our calculations yield 2.21 Å and 2.23 Å respectively for Si-Br bond lengths in SiH_3Br molecule and the bromine atop adsorption site on silicon (111) surface in excellent agreement with the corresponding experimental values of 2.210Å for the molecule and[2] (2.22+0.01)Å and[3] (2.17+0.04)Å for the surface. Predictions have also been made for the ^{79}Br nuclear quadrupole coupling constants and the local density of states for the chemisorbed system.

1.C. Newman et.al., J. Chem. Phys. 25, 855 (1945).
2.G. Materlik and J. Zegenhagen, Phys. Lett. 104A, 47 (1984).
3.M.J. Bedzyk et.al., J. Vac. Sci. Technol. 20, 634(1982).

14:42
EJ 2 Self-Consistent Pseudofunction Method Calculations of Band Structure for Si Surfaces.* D. D. CHAMBLISS and T. N. RHODIN, Cornell U., R. V. KASOWSKI and M.-H. TSAI, E.I. duPont.--The self-consistent pseudofunction method for thin-film band structure calculations is presented in terms of its applicability to the surfaces of semiconductors. This method is a significant improvement on the SCF-EMTO method[1] in that the basis functions contain accurate radial solutions well beyond the muffin-tin radius. Energy bands from self-consistent calculations on ideal 4-layer and 8-layer Si(111) and Si(100) films are presented and compared with pseudopotential-method results.[2]

*Supported by NSF DMR 8217227-A01 and NSF DMR 8303742.

[1] R. V. Kasowski and M.-H. Tsai, Phys. Rev. B29, 1043 (1984).
[2] M. Schlüter, J. R. Chelikowsky, S. G. Louie and M. L. Cohen, Phys. Rev. B12, 4200 (1975).

14:54
EJ 3 Surface States of Cleaved (111) Si and Ge Observed by Tunneling T. PENNEY, W. A. THOMPSON, and R. H. KOCH IBM Yorktown Heights, NY --Clean interfacial surfaces of either degenerately doped Si or Ge have been prepared by cleaving bars under liquid He. The bar is spring loaded so that after cleaving, the freshly prepared interfacial surface remains in contact producing a homojunction. The double Schottky barriers at the cleaved interface which naturally occur due to charge exchange between the bulk and surface states deep in the gap serve as the tunneling barrier. We have observed very sharp (<1mV) structure in the tunneling resistance spectra extending several tens of mV in bias voltage. This structure is symmetric for a given sample but differs in detail from sample to sample. This structure is consistent with a model in which, with increasing bias voltage, surface states initially above the Fermi energy are successively filled. As each state is filled, the added charge at the interface inhibits the tunneling current nearby.

15:06
EJ 4 Surface Electronic Structure of Si(111)7x7 and Si(111)$\sqrt{3}$x$\sqrt{3}$:Al from Angle-Resolved Photoemission. R. I. G. UHRBERG*, G. V. HANSSON and J. M. NICHOLLS, Linkoping Inst. of Techn. — The Si(111)7x7 surface has three surface states at ~ 0.2 eV (S1), ~ 0.8 eV (S2) and ~ 1.8 eV (S3) below EF. In the present work we report a dispersion of ~ 0.3 eV for the S3 surface state in the 1x1 surface Brillouin zone (SBZ). The Si(111)$\sqrt{3}$x$\sqrt{3}$:Al surface is found to have similar electronic structure to Si(111)7x7. The main difference is that the S2 surface state is missing, while we find two surface states, A1 and A3, qualitatively similar to the S1 and S3 surface states. A3 has higher emission intensity and a larger bandwidth (~ 0.65 eV) compared to S3. The observed dispersion for A3 follows the 1x1 SBZ instead of the expected $\sqrt{3}$x$\sqrt{3}$ SBZ. A recent calculation [1] of the surface state bands for Si(111)$\sqrt{3}$x$\sqrt{3}$:Al shows two filled surface state bands in the energy region where A3 is found. These calculated bands are consistent with the experimental results if one assumes that only one band at a time is observed in photoemission.

*Present Address: Xerox Palo Alto Res. Ctr.

1. J. E. Northrup, Phys. Rev. Lett. 53, 683 (1984)

**Submitted by R.D. Bringans

is there evidence for separate (almost resolved) "white lines" in the spectra reminiscent of the core-level spectra of rare earth mixed-valent materials. Results on intermetallic compounds of the form: U_2T, UT_2, UT_3 and UT_5, where T= 3d, 4d and 5d transition metals and U_xX_y compounds were X = S, Be, Al, Si, Ga, Sn, and Pd. In particular all of the U-heavy-fermion-superconductors will be covered. Evidence for valence changes and bandwidth changes in selected compound series will be discussed along with experimental finite optical thickness effects.

Work supported by the DOE under grant number DE-FG05-84ER45021.

15:06

NJ 9 The Effects of Diluting Mixed Valent Ce Systems with Y, La, Lu and Th, T.MIHALISIN, R. SELIM, Temple U.* Y. S. CHAUG and R. D. PARKS, New York U.** -- The effect of diluting Ce with Y, La, Lu or Th on the valence of Ce in mixed valent compounds has been investigated via L_{III} absorption measurements. The effects of dilution by Th has been determined for $CeRh_3$, $CeRu_2$, $CeNi_2$ and $CePd_3$. In all cases Th decreases the valence of Ce except in the case of $CeRh_3$ where Ce remains at the saturation valence value of 3.2. The effect of La dilution of $CeRu_2$ is also to lower the Ce valence. The effects of Y dilution in $CeNi_2$ and Lu dilution in $CePd_3$ and $CeRh_3$ have also been determined. These results along with complementary investigations by others will be discussed in terms of electron counting and lattice pressure effects.
* Supported by NSF DMR-8219782.
**Supported by NSF DMR-8202726.

15:18

NJ 10 L_{III} Absorption Studies of $Ce(Ni,Co)_2$, $(Ce,Y)Ni_2$ and $(Ce,Y)Co_2$, B. ANDRAKA, J. TIMLIN and T. MIHALISIN, Temple U. --E. KEMLY and M. CROFT, Rutgers U.-- L_{III} absorption measurements of $CeNi_2$ and related pseudo-binaries $Ce(Ni,Co)_2$, $(Ce,Y)Ni_2$ and $(Ce,Y)Co_2$ have been made in order to determine the valence of Ce and how it is altered by substituting Co for Ni or Y for Ce. We find that the valence increases as one moves from $CeNi_2$ to $Ce(Ni_{.2}Co_{.8})_2$ or from $CeNi_2$ to $Ce_{.2}Y_{.8}Ni_2$ and saturates at about the same value in both cases. On the other hand the substitution of Y for Ce in $CeCo_2$ (i.e., $Ce_{1-x}Y_xCo_2$) does not change the valence of Ce which is already at the saturation value (in pure $CeCo_2$). These results will be compared to recent studies[1] of the behavior of thermodynamic properties in these systems.
*Supported by NSF DMR-8219782.
1. B. Andraka, J. Timlin and T. Mihalisin, J. Mag. Mag. Mat. 47 and 48, (1985).

15:30

NJ 11 $Ce(Pd,Rh)_3$, $Zr(Pd,Rh)_3$ and Related Pseudo-binaries: A Case for Tetravalent Cerium, A. HARRUS, R. SELIM and T. MIHALISIN, Temple U.* -- The upper limit of the valence of Ce remains a controversial issue. The valence determined by L_{III} absorption never exceeds a "saturation" value of 3.2 to 3.3. We are able to predict the mixed valent-trivalent and mixed valent-"saturated" valent border concentrations for $Ce(Pd,Rh)_3$, $Ce(Pd,Ag)_3$ and $(Ce,M)Pd_3$ with M = La, Y, Sc, and Th, if we assume that the saturation valence value is 4 and that each electron added via alloying is added to the Ce ions. This prediction is based on the concept put forward by Harris and coworkers[1] that in this system the Cu_3Au structure is stable only up to a maximum number of electrons per cell. $CePd_3$ and the related pseudo-binaries listed above form the only system for which the model gives accurate predictions. This may be due to the f electron density of states far exceeding that of the d electrons in $CePd_3$ but not in other systems such as $CeNi_2$, $CeRh_2$, etc.
*Supported by NSF DMR-8219782.
1. J. M. Pountney, J. M. Winterbottom and I. R. Harris, in: Rare Earths and Actinides, 1977; ed. by W. D. Corner and B. K. Tanner, The Inst. of Phys., London (1978) p.45.

15:42

NJ 12 Measurement of the Optical Conductivity of $CePd_3$ from 0.3 to 500 meV. B. C. WEBB, and A. J. SIEVERS, Cornell U.*--The far infrared reflectivity of $CePd_3$ has been measured by optical and quasioptical techniques between 4 and 300 K over the range 0.3 to 500 meV. These measurements extend the energy range by two orders of magnitude over that previously reported[1] and map out the entire spectral region of the low temperature absorptivity anomaly. We find that the anomaly is too large to be compatible with simple conduction electron scattering off a resonant level near the Fermi energy. The real part of the complex conductivity, which is obtained from a Kramers-Kronig analysis of the absorptivity data over a large frequency interval, is dominated by two frequency dependent features: a narrow Drude component which shows a 70 fold decrease as energy increases to 3 meV and a broad Lorentzian component centered at 200 meV.
*Supported by NSF and AFOSR.
[1]F. E. Pinkerton et al., Phys. Rev. B 29, 609 (1984).

15:54

NJ 13 Electronic Structure of NiO and NiS. G.A. SAWATZKY, Univ. of Groningen,, J.W. ALLEN and J.C. MIKKELSEN, Xerox Palo Alto Res. Ctr. — Photoemission (PES) and bremstrahlung isochromat spectroscopy (BIS) data on cleaved single crystals of NiO and NiS are presented and compared to predictions from band theory and from a local cluster Green's-function approach to the Anderson Hamiltonian. In contrast to band theory predictions[1] the band gap of NiO is found[2] to be large, ~4.3 eV, but not determined solely by the even larger d-d Coulomb interaction U~7.9 eV which separates the d^7 PES and the d^9 BIS peaks. Other states of the type (d^8. ligand hole) fall inside this correlation gap, causing the charge transfer (c-t) gap to be much smaller and determined by the electronegativity of the ligand. We expect mixed valence for metallic NiS, i.e., that the c-t gap goes to zero, but that U remains large. This general picture appears to have application to the systematics of many transition metal compounds, as will be discussed.
1. K. Terakura, A.R. Williams, T. Oguchi and J. Kubler, Phys. Rev. Lett. 52, 1830 (1984).
2. G.A. Sawatzky & J.W. Allen, Phys. Rev. Lett 53, 2339 (1984).

16:06

NJ 14 Susceptibility of $Ce_{1-x}Y_xCo_2$: A System with Strongly Varying d-Electron Spin Fluctuations, J. TIMLIN and T. MIHALISIN, Temple U.* -- We have measured the susceptibility of $Ce_{1-x}Y_xCo_2$ samples with x=0 to 1, from 2K to 300K. Large variations in the magnitude of the susceptibility at 300K are seen with χ(300) for YCo_2 ~4memu/mole and χ(300) for $CeCo_2$ ~1memu/mole. Moreover, the temperature dependence of χ across the series changes dramatically. For $0.4<x<1$, χ increases with increasing temperature over the entire range. But for $x<0.4$, χ decreases with increasing temperatures. At the lowest temperature χ is proportional to T^2 for all samples. Evidence will be presented to support the idea that d electron spin fluctuations are responsible for this behavior across the entire series from YCo_2 to $CeCo_2$. That is, f electron contributions to χ are negligible, even in $CeCo_2$. Comparisons to theory will be presented.
*Supported by NSF DMR-8219782.

16:18

NJ 15 Ce Valence and Superconductivity in the (Ce,Th) Ru_2 System, A. ANBALAGAN and T. MIHALISIN, Temple U.* -- We have measured the normal state resistivity and superconducting T_c's of $Ce_{1-x}Th_xRu_2$ samples from x=0 to 1. The effect of diluting presumably mixed valent Ce with tetravalent Th differs remarkably from prior results obtained for $Ce_{1-x}La_xRu_2$, where one dilutes Ce with trivalent La, and for $La_{1-x}Th_xRu_2$ where one dilutes trivalent La with

VI. PUBLICATIONS AND DEGREES AWARDED (1981-1985)

A) Publications

"Broadband Surface Electromagnetic Wave Spectroscopy," Z. Schlesinger and A. J. Sievers, Surface Science 102, L29-34 (1981).

"Far Infrared Surface Electromagnetic Wave Propagation Lengths," Z. Schlesinger, B. C. Webb and A. J. Sievers, Bull Am. Phys. Soc. 26, 358-359 (1981).

"Attenuation and Coupling of Far Infrared Surface Plasmons," Z. Schlesinger, B. C. Webb and A. J. Sievers, Solid State Communications 39, 1035-1039 (1981).

"Intraband Magneto-optical Studies of InSb-NiSb Eutectic," A. K. Chin and A. J. Sievers, Jour. Appl. Phys., 52, 7380 (1981).

"Spectroscopy with IR Surface Plasmons," A.J. Sievers, Bull. Amer. Phys. Soc. 27, 262 (1982).

"Dielectric Function of Silver by Surface Plasmons," H. Gugger, J. D. Swalen, A. J. Sievers, Bull. Amer. Phys. Soc. 27, 343 (1982).

"Influence of the Depolarization Field on Linewidth and Structure of Adsorbate Vibrational Mode Spectra," Z. Schlesinger and A. J. Sievers, Bull. Amer. Phys. Soc. 27, 410 (1982).

"Dipole-Dipole Coupling in Adsorbate Vibrational Mode Spectra," Z. Schlesinger and A. J. Sievers, Vibrationals at Surface, Asilomar, California, September, 1982.

"IR Surface Plasmon Attenuation Coefficients for Ag and Au Films," Z. Schlesinger and A. J. Sievers, Solid State Commun. 43, 671 (1982).

"IR Surface Plasmon Attenuation Coefficients for Ge-coated Ag and Au Metals," Z. Schlesinger and A. J. Sievers, Phys. Rev. B26, 6444 (1982).

"Shallow Traps and the D^- center in Ge:Sb; Far-infrared photoconductivity studies below 1K," E. A. Schiff, Philosophical Mag. B 45, 69 (1982).

"IR Surface Plasmon Spectroscopy," in Ellipsometry and Other Optical Methods for Surface and Thin Film Analysis, F. Abeles ed., Journal de Physique, Colloque C-10 44, 13 (1983) with Z. Schlesinger.

"IR Spectroscopy with Surface Electromagnetic Waves," in Dynamics of Interfaces, L. Dobrzynski ed., Journal de Physique, Colloque C-5, 45 167 (1984) with Z. Schlesinger and Y. J. Chabal.

"Non-linear IR Properties of an LO Phonon in Thin $KReO_4$ Films," Physical Review B 28, 4863 (1983), with L. H. Greene and Z. Schlesinger.

"IR Study of the Adsorption of Oxygen and Hydrogen on W(100)," Bull. Amer. Phys. Soc. 29 (1984) with L. H. Greene and Z. Schlesinger.

"Observation of an Index of Refraction Induced Change in the Drude Parameters of Ag Films," Phys. Rev. B 30, 4189 (1984), with H. Gugger, M. Jurich and J. D. Swalen.

"Infrared Surface Plasmon Interferometry on Clean Metal Surfaces," L. M. Hanssen, D. M. Riffe and A. J. Sievers, Forty-Fourth Annual Conference on Physical Electronics, Princeton, N.J. (1984) D-10.

"The Effect of Melting of the Metallic Component on the Anomalous Far-Infrared Absorption of Superconducting Sn Particle Composites," W. A. Curtin, R. C. Apitzer, N. W. Ashcroft and A. J. Sievers, Phys. Rev. Letters 54, 1071 (1985).

"The Mie Resonance for Spherical Metal Particles in an Anistropic Dielectric," R. P. Devaty and A. J. Sievers, Phys. Rev. B 31 2427 (1985).

"Absorptivity of $CePd_3$ from 5 to 400 meV," B. C. Webb, A. J. Sievers and T. W. Mihalisin, Jour. of Applied Physics 57, 3134 (1985).

"Evaporated Epitaxial Chronium Films," J. G. Cook, Thin Solid Films 129, L57 (1985).

"Observability of Quantum Size Effects in Small Metal Particles by Absorption Spectroscopy," R. P. Devaty and A. J. Sievers, Bull. Amer. Phys. Soc. 30, 307 (1985).

"First SEW Observation of Surface Reconstruction on W(100)," D. M. Riffe, L. M. Hanssen and A. J. Sievers, Bull. Amer. Phys. Soc. 30, 361 (1985).

"Measurement of the Optical Conductivity of $CePd_3$ from 0.3 to 500 meV," B. C. Webb and A. J. Sievers, Bull. Amer. Phys. Soc. 30, 638 (1985).

"2DEG in $In_{0.53}Ga_{0.47}As$/InP Heterostructures Grown by Atmospheric MOCVD," L. D. Zhyu, P. Sulewski, K. T. Chan, J. M. Ballantyne and A. J. Sievers, Bull. Amer. Phys. Soc. 30, 209 (1985).

B) Degrees Awarded and Thesis Abstracts

Zack Schlesinger, Ph.D. 1982 Cornell University.

Dr. Schlesinger is now a Research Scientist at IBM Research Labs, Yorktown Heights.

Robert P. Devaty, Ph.D. 1983 Cornell University

Dr. Devaty is now an Assistant Professor in the Physics Department at University of Pittsburgh.

Leonard M. Hanssen, Ph.D. 1985 Cornell University

Dr. Hanssen is now a Research Scientist at T.R.W. Redondo Beach, California.

EXPLORING THE OPTICAL PROPERTIES OF DIELECTRIC COATED METALS WITH INFRARED SURFACE PLASMONS

Zack Schlesinger, Ph.D.
Cornell University, 1982

The surface plasmon (SP) is a coupled photon-plasmon mode which exists at metal surfaces. Unlike other bound electromagnetic modes SP's are not confined to a particular region of space by geometrical boundaries. Instead their field profiles are determined by the dielectric properties of the supporting media and their degree of confinement is very sensitive to small changes in phase velocity. In this thesis the optical and physical properties of propagating infrared SP's are explored both theoretically and experimentally to determine the usefulness of this high resolution, surface sensitive probe.

With ir laser sources a comprehensive study of SP propagation has been carried out at 84 cm^{-1} and 10^3 cm^{-1} using dielectric coatings to vary the degree of confinement of the SP mode. Strong linear coupling occurs at coating edges between SP and bulk modes. At 84 cm^{-1} SP excitation is inefficient and plane waves dominate the surface transmission signal, while at 1000 cm^{-1} interference between the SP and plane wave modes can be observed. A SP interferometer has been developed to measure the SP phase velocity. From SP phase velocity measurements at 1000 cm^{-1} the infrared mass of Ag and Au is determined.

The feasibility of using broadband infrared SP transmission spectroscopy to study the vibrational modes of molecules on metal surfaces has been demonstrated with the development of a dispersion compensating edge coupler. For $KReO_4$ coated metal samples the internal vibrational mode of the ReO_4^- molecules near 1000 cm^{-1} is used to compare the SP and surface reflection spectroscopy techniques. The integrated intensity of the absorption line is an order of magnitude larger with the SP transmission technique; however, the overall signal level is too low to make this a practical technique without further improvements in SP coupling efficiency.

G. P. Sievers

FAR INFRARED ABSORPTION BY SMALL SILVER PARTICLES

Robert Philip Devaty, Ph.D.
Cornell University, 1983

The anomalous enhancement by several orders of magnitude of the measured far infrared absorption coefficient of composite materials containing small metal particles with respect to the predictions of simple models has defied understanding largely due to a lack of well-characterized and controlled samples. To address some of the most basic questions about the effect, a novel composite material--100Å diameter Ag particles imbedded in gelatin--was developed and investigated. The same material can be studied by both far infrared Fourier transform spectroscopy and transmission electron microscopy. The volume fraction, f, of Ag is adjustable and samples with either well-dispersed or agglomerated particles can be prepared.

The far infrared absorption coefficient was measured for a variety of samples and compared with the predictions of the Bruggeman effective medium model for Drude Ag particles imbedded in the absorbing gelatin host. Agreement between experiment and theory was obtained for samples containing well-dispersed particles with $f \leq 0.15$. Due to absorption by the gelatin, these data only imply a bound of a factor of one hundred on the maximum possible enhancement, although the results are consistent with no enhancement whatsoever.

Absorption by the particles dominates for samples with $f \leq 0.15$, but the measured absorption is never greater than the prediction of theory by more than a factor of about ten. For samples with $f < 0.05$ containing deliberately agglomerated particles, the absorption per particle was enhanced by up to a factor of ten with respect to samples with well-dispersed particles. Thus, composite material containing well-dispersed particles shows no evidence for anomalously enhanced absorption, but agglomerated particles are stronger absorbers of far infrared radiation.

An IR Surface Electromagnetic Wave Measurement of Hydrogen Adsorption and Surface Reconstruction of W(100)

Leonard M. Hanssen, Ph.D.

Cornell University, 1985

Both the clean and hydrogen covered W(100) surfaces are probed with an inhomogenous electromagnetic mode which is bound to the metal surface. This Surface Electromagnetic Wave (SEW) is generated from a plane wave spectrum by means of a grating which is directly etched into the metal surface. A second grating, spaced about 5 cm from the first, transforms the SEW back into a plane wave infrared beam.

Near room temperature, the temperature dependence of the magnitude of the SEW signal agrees with the Drude model prediction using the d.c. resistivity. At high temperatures (>1000K) however, the SEW signal is attenuated to such a large extent that plane wave radiation generated at the first grating can be detected as well. Since both kinds of waves are generated coherently and travel across the surface with different velocities, interference is observed. This first SEW interferometer on a clean metal surface is used to directly measure the real part of the dielectric function in the 10 μm wavelength region. The plasma frequency of W is determined to be $h\omega_p$=7.0±0.3eV, about 17% larger than that estimated from other less accurate optical techniques.

The first SEW spectrum of surface reconstruction has been observed upon hydrogen adsorption on a W(100) sample maintained near room temperature. The reconstruction of the W(100)-H surface is checked

and calibrated through LEED observations and thermal desorption measurements. The SEW signal is found to follow a sigmoid curve as a function of coverage. Intensity changes as large as 30% of the clean surface value occur as the state of the W(100)-H surface changes. This extreme sensitivity of the SEW attentuation length to surface reconstruction is shown to be consistent with changes in the diffuse surface scattering component of the conduction electron scattering time.

In addition to identifying the SEW signature associated with surface reconstruction of W(100)-H, it has been possible to identify the SEW absorption associated with the ν_1 vibrational mode of the hydrogen saturated W(100) surface. The absorption line is measured to be broad in frequency, FWHM=120 cm^{-1}, and of line strengh given by the effective dipole charge (e*/e)=0.07. These results are in agreement with previous EELS measurements but contradict an earlier SEW measurement where a narrow line was found.

VII. PROFESSIONAL PERSONNEL (1981-1985)

A. K. Chin	graduate student
R. P. Devaty	graduate student
L. H. Greene	graduate student
L. M. Hanssen	graduate student
Z. Schlesinger	graduate student
B. C. Webb	graduate student
A. J. Sievers	Professor in charge

END

FILMED

5-86

DTIC